NTNU – Trondheim
Norwegian University of
Science and Technology

Methods for Earthquake Analysis

Helge Dørheim

Civil and Environmental Engineering
Submission date: June 2012
Supervisor: Anders Rönnquist, KT
Co-supervisor: Ragnar Sigbjörnsson, KT

Norwegian University of Science and Technology
Department of Structural Engineering

Department of Structural Engineering
Faculty of Engineering Science and Technology
NTNU- Norwegian University of Science and Technology

ACCESSIBILITY

Open

MASTER THESIS 2012

SUBJECT AREA: Earthquake Engineering	DATE: June 2012	NO. OF PAGES: 90

TITLE:

Methods for Earthquake Analysis

BY:
Helge Dørheim

SUMMARY:

Based on the need for effective solutions of structures response to seismic loading, this thesis includes the theoretical background, and explanation of several methods. There are many theories in the community, but the ones chosen to be looked closer at here are Modal response spectrum analysis for symmetric and asymmetric plan structures, Modal Pushover Analysis for symmetric and asymmetric plan structures and Linear and Non-Linear Response History Analysis. The theory has been adapted from published papers and books on the topic.

The report is divided into three main sections, numerical methods for solving of dynamic problems, elastic analysis and inelastic analysis. The chapters on Elastic and Inelastic analysis are further divided into sections on symmetric and asymmetric plan.

Elastic analyses by hand calculations and SAP2000 have been performed on a 2D-frame, a SAP2000 Elastic Response spectrum analysis has been performed on a 3D-frame, and an inelastic modal pushover analysis in SAP2000 has been performed on a 2D frame.

The target for this inquiry is to discover advantages and disadvantages in the different methods and comparing them.

RESPONSIBLE TEACHER: Anders Rönnquist

SUPERVISOR(S): Anders Rönnquist, Ragnar Sigbjörnsson

CARRIED OUT AT: Department for Structural Engineering, NTNU

Norwegian University of Science and Technology
NTNU
Department of Structural Engineering

Master's Thesis for Stud techn. Helge Dørheim, Spring 2012

Methods for Earhquake Analysis

Earthquake design was introduced to land based Norwegian structures through NS 3491-12. This code was implemented as a transition into the new NS-EN 1998 Eurocode 8. This code demands that, with a few exceptions, all structures have to be controlled for earthquake load.

It is common practice to use elastic design even for seismic loading, and this may cause an unnecessary stiff building, and larger material costs. Using more advanced analysis methods allows for better use of the inelastic regions energy dissipating properties, giving more effective structures.

This thesis will investigate different analysis methods that are relevant for Norwegian structures, and go into the theory behind them.

Literature Study
- Elastic analysis of symmetric plan structures
- Elastic analysis of asymmetric plan structures
- Modal Pushover Analysis, symmetric plan structures
- Modal Pushover Analysis, asymmetric plan structures
- Numerical time integration methods
- Time History Analysis

Case study:
- Numerical models in SAP2000 for comparison of methods
- Compare with hand calculations

Supervisors: Anders Rönnquist and Ragnar Sigbjörnsson NTNU

The thesis is to be submitted to the Department of Structural Engineering by 11th of June 2012

Preface

This report is written as a Master's Thesis at the Department of Structural Engineering at the Norwegian University of Science and Technology. The report has been written over the course of 20 weeks during the spring semester of 2012 and should cover 30 credits.

In addition to the content of this report much time has been used on studying NS-EN-1998-1:2004, Eurocode 8, and work in CSi SAP2000, MATLAB, LaTeX and Microsoft Excel. Many hours were also spent reading papers and narrowing the scope of the thesis. Non-linear finite element methods have also been studied to understand and use the non-linear possibilities in CSi SAP2000 effectively. It has been a rewarding semester where I have learned a lot about earthquake analysis, individual work and myself.

I would like to present a thanks to my supervisor Anders Rönnquist for his help, and to my fellow students at room 2-66 for input and discussion. As a final remark I would also like to express my gratitude to my lecturers, Dr. Tam Larkin, Associate Professor Nawawi Chouw and Dr. Rolando Orense, at the University of Auckland who opened the door to earthquake engineering for me.

Helge Dørheim
Trondheim, Juni 2012

Abstract

Based on the need for effective solutions of structures response to seismic loading, this thesis includes the theoretical background, and explanation of several methods. There are many theories in the community, but the ones chosen to be looked closer at here are Modal response spectrum analysis for symmetric and asymmetric plan structures, Modal Pushover Analysis for symmetric and asymmetric plan structures and Linear and Non-Linear Response History Analysis. The theory has been adapted from published papers and books on the topic.

The report is divided into three main sections, numerical methods for solving of dynamic problems, elastic analysis and inelastic analysis. The chapters on Elastic and Inelastic analysis are further divided into sections on symmetric and asymmetric plan.

Elastic analyses by hand calculations and SAP2000 have been performed on a 2D-frame, a SAP2000 Elastic Response spectrum analysis has been performed on a 3D-frame, and an inelastic modal pushover analysis in SAP2000 has been performed on a 2D frame.

The target for this inquiry is to discover advantages and disadvantages in the different methods and comparing them.

Sammendrag

Med utgangspunkt i behovet for en effektiv måte å løse konstruksjoners respons til seismisk last har denne rapporten utforsket flere metoder for løsning. I tidligfasen ble det sett på flere analysemetoder, før de ble begrenset ned til modal responsspektrumanalyse for symmetriske og usymmetriske plan, modal pushover analyse for symmetriske og usymmetriske plan, samt lineær og ikke-lineær tidshistorie. Underliggende teori og forklaring av de utvalgte metodene er inkludert. Teorien er bearbeidet fra bøker og publiserte artikler om emnet.

Rapporten er delt opp i tre hoveddeler, den første beskriver numeriske metoder for løsning av dynamiske problemer, den andre elastisk analyse og den tredje inelastisk analyse. Kaptilene om elastisk og inelastisk analyse er videre delt mellom symmetrisk og usymmetriske plan.

Elastisk analyse gjort ved håndberegninger og i SAP2000 har blitt utforørt på en 2D-ramme, en SAP2000 elastisk responsspektrumanalyse har blitt utført på en 3D-ramme og en inelastisk modal pushover analyse har blitt utført på en 2D-ramme.

Målet med oppgaven er å se på fordeler og ulemper med de forskjellige metodene, og dermed gi et forslag på hvilke metoder som bør brukes i gitte situasjoner.

Contents

1 Introduction **1**

2 Numerical Methods to Solve Dynamic Problems **3**
- 2.1 Direct Integration . . . 3
  - 2.1.1 Newmark Method . . . 4
  - 2.1.2 Hilber-Hughes-Taylor . . . 9
  - 2.1.3 Non-linear Newmarks Method . . . 9
- 2.2 Numerical Damping . . . 12

3 Elastic Analysis **15**
- 3.1 Symmetric Plan Buildings . . . 15
  - 3.1.1 Modal Analysis . . . 15
  - 3.1.2 Modal Response Contributions . . . 17
  - 3.1.3 Response Spectrum Analysis Procedure . . . 21
  - 3.1.4 Elastic Analysis of a 2D-frame . . . 22
- 3.2 Asymmetric Plan Buildings . . . 27
  - 3.2.1 One Story, Two Way Asymmetric System . . . 28
  - 3.2.2 Multi-story One Way Asymmetric System . . . 30
  - 3.2.3 Response Spectrum Analysis of an Asymmetric Plan Structure . . . 34

4 Inelastic Analysis **39**
- 4.1 Response History Analysis . . . 42
- 4.2 Uncoupled Modal Response History Analysis . . . 42
- 4.3 Properties of the nth Mode Inelastic SDOF-system and Pushover Curve . . . 44
- 4.4 Modal Pushover Analysis . . . 45
  - 4.4.1 Modal Pushover Analysis of a 2D Frame . . . 46
- 4.5 Modal Pushover Analysis for Asymmetric Plan Systems . . . 54
  - 4.5.1 Elastic Systems . . . 54
  - 4.5.2 Inelastic Systems . . . 54

5 Eurocode 8 **59**
- 5.1 Non-Linear Static Analysis (Pushover Analysis) . . . 59
  - 5.1.1 Determination of the Target Displacement for Non-linear Static Analysis (Pushover Analysis) . . . 60

6 Conclusion **63**

7 Further Work **65**

A Response Spectrum **67**

B Elastic Analysis - Matlab **69**

C Correlation Coefficient **73**

List of Figures

2.1 Comparison of implicit and explicit methods [1] 4
2.2 Constant Acceleration Method and Linear Acceleration Method 5
2.3 El Centro Ground Motion [4] 8
2.4 Displacement history 8
2.5 Illustration of secant and tangent stiffness [3] 10
2.6 Illustration of numerical errors [3] 11
2.7 Illustration of iterations [3] 11

3.1 Schematic description of modal response [3] 19
3.2 Correlation Factor [3] 21
3.3 Multi-story Frame 23
3.4 Normalized mode shapes 24
3.5 Response spectrum for El Centro ground motion for 5% damping 24
3.6 Comparison of time history of base shear for Linear Modal History and Linear Direct Integration 27
3.7 Illustration of asymmetric system 28
3.8 Imposed unit displacements to construct k [3] 29
3.9 SAP2000 System 35
3.10 Correlation coefficient for 5% damping 37
3.11 Correlation coefficient for 20 % damping 37
3.12 Envelope of deformation for Linear Modal History Analysis in Y-direction . . 38

4.1 Global Pushover Curve of 20 Story Building LA, with and without P-delta [8] 40
4.2 Effects of P-delta effects [3] 40
4.3 Influence on story drifts by modelling [3] 41
4.4 Statistical values of story drift demands for LA-Structure M2 Model [10] . . 41
4.5 Modal Decomposition of the roof displacement [9] 43
4.6 Conceptual explanation of uncoupled modal RHA of inelastic MDOF systems [9] 44
4.7 Hinge Properties 47
4.8 Mode shapes 1 through 3 47
4.9 Pushover-curves for mode 1,2 and 3 49
4.10 Plastic hinge formation 49
4.11 Force Displacement Curves for mode 1,2 and 3 50
4.12 Design Spectrum from EC8 for ground acceleration 0.3188g and 0.4782g . . . 51
4.13 Floor Displacement comparison NL-RHA and MPA 52
4.14 Development of plastic hinges, NL-RHA to the left, and MPA-mode 1 to the right 53

4.15 Plan of asymmetric plan building [12] 55
4.16 Mode shapes of systems [12] 56
4.17 Floor Displacements and story drift demands for symmetric plan, U1, U2 and U3 [12] 57
4.18 Floor Displacement and story drift comparison of CQC and ABSSUM [12] . 58

5.1 Determination of the idealized elasto-perfectly plastic force displacement relationship [11] 61

List of Tables

3.1 Comparison of modal periods 26
3.2 Comparison of base shear and roof displacement 26
3.3 Modal Static Responses [3] 33
3.4 Modal Periods 36
3.5 Comparison of CQC and SRSS 36

4.1 Modal Participation Factors 48
4.2 Comparison of elastic and inelastic periods 50
4.3 Modal Pushover Analysis Results 51
4.4 Base Shear comparison MPA and NL-RHA 52

Chapter 1

Introduction

When the new NS 1998 Eurocode 8 was introduced, it meant that most Norwegian structures had to be designed for earthquake loading. Historically these kind of designs were all done in the elastic range, but this is very ineffective when it comes to seismic loading. The reason for this is the large energy dissipation that can be taken advantage of when structural members enter the inelastic range.

The use of elastic analysis can cause the building to become unnecessary stiff, giving two main drawbacks, number one: that more, and stronger, materials are needed, and number two: the use of more and stronger materials increases weight, again causing more forces, again demanding a stronger structure. The consequence for this is of course a higher price.

When allowing the structure to enter the inelastic region in the right areas, money can be saved because of lower material costs and lower weight, again reducing forces. There are obviously large challenges to this method of design. It demands a lot from the model used, and if the wrong place yields, it could cause major damage.

This thesis will investigate several methods for analysis of seismic loading on structure, both elastic and inelastic, discussing their advantages and disadvantages.

Chapter 2

Numerical Methods to Solve Dynamic Problems

This chapter contains the theory used to numerically solve the response to an acceleration time history. It will describe Newmarks method, which is used to create the displacement time history from El Centro ground motion through a MATLAB-script. The Hilber-Hughes-Taylor will be presented, which is used in SAP2000 for time history analysis. Mass- and stiffness-proportional damping, also used by SAP2000 will be described.

2.1 Direct Integration

This section will present the difference between implicit and explicit methods and general theory behind the Newmark method and Hilber-Hughes-Taylor method. The theory in this section is obtained from lecture notes from TKT4197 Non-linear Finite Element Analysis by Kjell Magne Mathisen [1] and Civil 720 Earthquake Engineering by Tam Larkin [2] and Dynamics of Structures by Chopra [3].

Direct integration methods are used to solve an initial value problem using step-by-step integration in time. This means that the displacements, U_0 and velocities $\dot{u}_0$, are assumed to be known at a given time, $t = 0$. The time period where a result is wanted is then divided into time increments and the integration method solves approximate solutions at each of these time steps. In earthquake analysis, the acceleration is assumed to vary in a given way during the time interval, and then integrated to find velocities and displacements at the next time step.

The direct integration methods are divided into two main groups, implicit and explicit.

- Explicit Methods: The displacement at time t_{n+1}, U_{n+1}, is obtained explicitly from the equilibrium conditions at one or more of the preceding steps, without solving an equation system. Hence: Unknown values are found based on the information already known. If data from only one time-step is used, it is a single step method, while a method using data from two steps back is called a two step method. Explicit methods are conditionally stable, meaning that there is a critical time step Δt_{cr} that causes the process to become unstable if exceeded. This means that a large number of time-steps

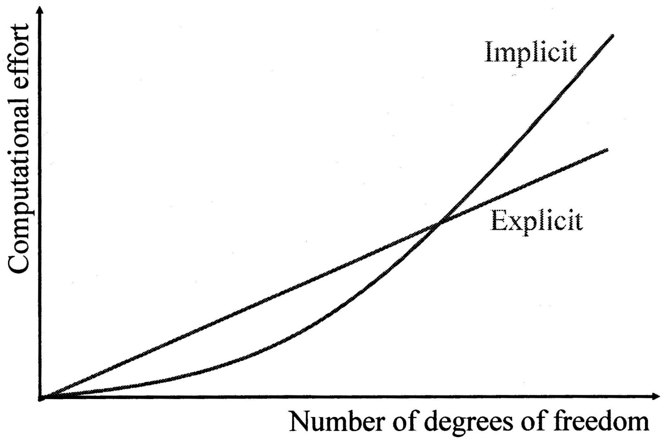

Figure 2.1: Comparison of implicit and explicit methods [1]

are needed, but a lumped mass matrix will increases the speed of which each step is executed.

- Implicit methods: These methods finds the displacement u_{n+1} implicitly from the equilibrium conditions at time t_{n+1}, hence needing equation solving. Implicit methods are unconditionally stable, meaning that they stay stable for any Δt. The accuracy will nonetheless decrease with increasing Δt.

As a summary it can be said that an explicit method requires many steps, but at low cost per step, while an implicit method requires fewer steps, but the cost per step is higher. This means that for responses dominated by high frequency modes, with a need for small time steps, like wave propagation problems from blasts or impacts calls for an explicit method, while structural dynamic problems with a limited time range and no need for small time steps calls for an implicit method. Figure 2.1 compares the computational effort for implicit and explicit methods.

2.1.1 Newmark Method

In the Journal of the Engineering Mechanics Division in 1959 N.M. Newmark developed a group of time stepping method based on the assumptions in equations (2.1a) and (2.1b)

$$\dot{u}_{n+1} = \dot{u} + \Delta t[\gamma \ddot{u}_{n+1} + (1-\gamma)\ddot{u}_n] \tag{2.1a}$$

$$u_{n+1} = u_n + \Delta t \dot{u}_n + \frac{\Delta t^2}{2}[2\beta \ddot{u}_{n+1} + (1-2\beta)\ddot{u}_n] \tag{2.1b}$$

The two special cases, constant average and linear acceleration methods will be looked at here. The methods are illustrated in figure 2.2 and the coefficients are derived as follows

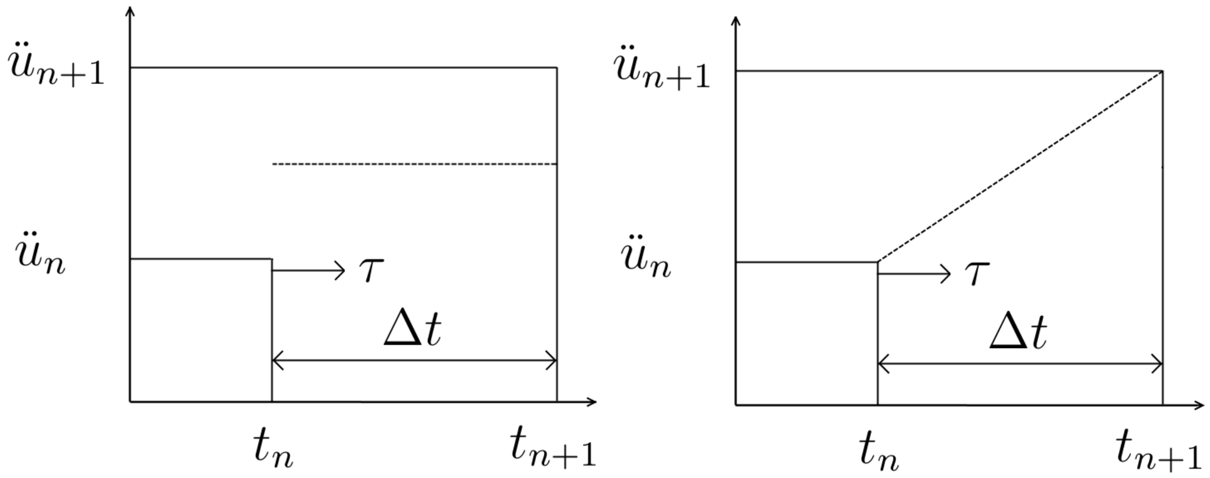
$\ddot{u}_{n+1}$
$\ddot{u}_n$
τ
Δt
t_n
t_{n+1}
$\ddot{u}_{n+1}$
$\ddot{u}_n$
τ
Δt
t_n
t_{n+1}

Figure 2.2: Constant Acceleration Method and Linear Acceleration Method

Constant Acceleration

$$\ddot{u}(\tau) = \frac{1}{2}(\ddot{u}_n + \ddot{u}_{n+1}) \tag{2.2}$$

$$\dot{u}_{n+1} = \dot{u}_n + \int\limits_t^{t+\Delta t} \ddot{u}(t)dt \tag{2.3}$$

$$\dot{u}(\tau) = \dot{u}_n + \frac{\tau}{2}(\ddot{u}_n + \ddot{u}_{n+1}) \tag{2.4}$$

$$\dot{u}_{n+1} = \dot{u}_n + \frac{\Delta t}{2}(\ddot{u}_n + \ddot{u}_{n+1}) \tag{2.5}$$

$$u_{n+1} = u_n + \int\limits_t^{t+\Delta t} \dot{u}(t)dt \tag{2.6}$$

$$u(\tau) = u_n + \dot{u}_n\tau + \frac{\tau^2}{4}(\ddot{u}_n + \ddot{u}_{n+1}) \tag{2.7}$$

$$u_{n+1} = u_n + \dot{u}_n\Delta t + \frac{(\Delta t)^2}{4}(\ddot{u}_n + \ddot{u}_{n+1}) \tag{2.8}$$

This shows that Constant Average Acceleration gives $\gamma = \frac{1}{2}, \quad \beta = \frac{1}{4}$

Linear Acceleration

$$\ddot{u}(\tau) = \ddot{u}_n + \frac{\tau}{\Delta t}(\ddot{u}_{n+1} - \ddot{u}_n) \tag{2.9}$$

$$\dot{u}_{n+1} = \dot{u}_n + \int\limits_{t}^{t+\tau} \ddot{u}(\tau) d\tau \tag{2.10}$$

$$\dot{u}(\tau) = \dot{u}_n + \ddot{u}_n \tau + \frac{\tau^2}{2\Delta t}(\ddot{u}_{n+1} - \ddot{u}_n) \tag{2.11}$$

$$\dot{u}_{n+1} = \dot{u}_n + \frac{\Delta t}{2}(\ddot{u}_{n+1} + \ddot{u}_n) \tag{2.12}$$

$$u_{n+1} = u_n + \int\limits_{t}^{t+\Delta t} \dot{u}(t) dt \tag{2.13}$$

$$u(\tau) = u_n + \dot{u}_n \tau + \ddot{u}_n \frac{\tau^2}{2} + \frac{\tau^3}{6\Delta t}(\ddot{u}_{n+1} - \ddot{u_n}) \tag{2.14}$$

$$u_{n+1} = u_n + \dot{u}\Delta t + \ddot{u}_n \frac{(\Delta t)^2}{2} + \frac{(\Delta t)^2}{6}(\ddot{u}_{n+1} - \ddot{u}_n) \tag{2.15}$$

$$u_{n+1} = u_n + \dot{u}\Delta t + (\Delta t)^2 \Big(\frac{1}{6}\ddot{u}_{n+1} + \frac{1}{3}\ddot{u}_n\Big) \tag{2.16}$$

Linear Acceleration gives $\gamma = \frac{1}{2}, \quad \beta = \frac{1}{6}$

These parameters define the stability, variation of acceleration over a time step, amount of algorithmic damping and the accuracy of the method.

The incremental quantities shown in equation (2.17) are not necessary for linear problems, but provides a practical extension to non-linear systems.

$$\begin{gathered} \Delta u_n \equiv u_{n+1} - u_n \quad \Delta \dot{u}_n \equiv \dot{u}_{n+1} - \dot{u}_n \quad \Delta \ddot{u}_n \equiv \Delta \ddot{u}_{n+1} - \ddot{u}_n \\ \Delta p_n \equiv p_{n+1} - p_n \end{gathered} \tag{2.17}$$

Combining equation (2.1a), equation (2.1b) and equation (2.17) gives

$$\Delta \dot{u}_n = (\Delta t)\ddot{u}_n + (\gamma \Delta t)\Delta \ddot{u}_n \quad \Delta u_n = (\Delta t)\dot{u}_n + \frac{(\Delta t)^2}{2}\ddot{u}_n + \beta(\Delta t)^2 \Delta \ddot{u}_n \tag{2.18}$$

Solving the second for $\Delta \ddot{u}_n$ provides

$$\Delta \ddot{u}_n = \frac{1}{\beta(\Delta t)^2}\Delta u_n - \frac{1}{\beta \Delta t}\dot{u}_n - \frac{1}{2\beta}\ddot{u}_n \tag{2.19}$$

When equation (2.19) is substituted into the first part of equation (2.18) the expression in equation (2.20) is obtained

$$\Delta \dot{u}_n = \frac{\gamma}{\beta \Delta t}\Delta u_n - \frac{\gamma}{\beta}\dot{u}_n + \Delta t\Big(1 - \frac{\gamma}{2\beta}\Big)\ddot{u}_n \tag{2.20}$$

This is then substituted into the incremental equation of motion

$$m\Delta\ddot{u}_n + c\Delta\dot{u}_n + k\Delta u_n = \Delta p_n \tag{2.21}$$

This provides

$$\begin{gathered}\left(k + \frac{\gamma}{\beta\Delta t}c + \frac{1}{\beta(\Delta t)^2}m\right)\Delta u_n = \\ \Delta p_n + \left(\frac{1}{\beta\Delta t}m + \frac{\gamma}{\beta}c\right)\dot{u}_n + \left[\frac{1}{2\beta}m + \Delta t\Big(\frac{\gamma}{2\beta} - 1\Big)c\right]\ddot{u}_n\end{gathered} \tag{2.22}$$

Then the notations $\hat{k}$ and $\hat{p}_n$ are introduced as

$$\begin{aligned}\hat{k} &= \left(k + \frac{\gamma}{\beta\Delta t}c + \frac{1}{\beta(\Delta t)^2}m\right) \\ \hat{p}_n &= \Delta p_n + \left(\frac{1}{\beta\Delta t}m + \frac{\gamma}{\beta}c\right)\dot{u}_n + \left[\frac{1}{2\beta}m + \Delta t\Big(\frac{\gamma}{2\beta} - 1\Big)c\right]\ddot{u}_n\end{aligned} \tag{2.23}$$

The incremental displacement is then calculated

$$\Delta u_n = \frac{\Delta\hat{p}_n}{\hat{k}} \tag{2.24}$$

When Δu_n is found equations (2.20) and (2.19) can compute $\Delta\dot{u}_n$ and $\Delta\ddot{u}_n$ respectively. These values are then put into equation (2.17) to find $u_{n+1}, \dot{u}_{n+1}$ and $\ddot{u}_{n+1}$.

This method has been used to compute the response of a SDOF system with period T=2 seconds to the El Centro Ground Motion. The ground motion and system displacements are shown in figures 2.3 and 2.4, respectively.

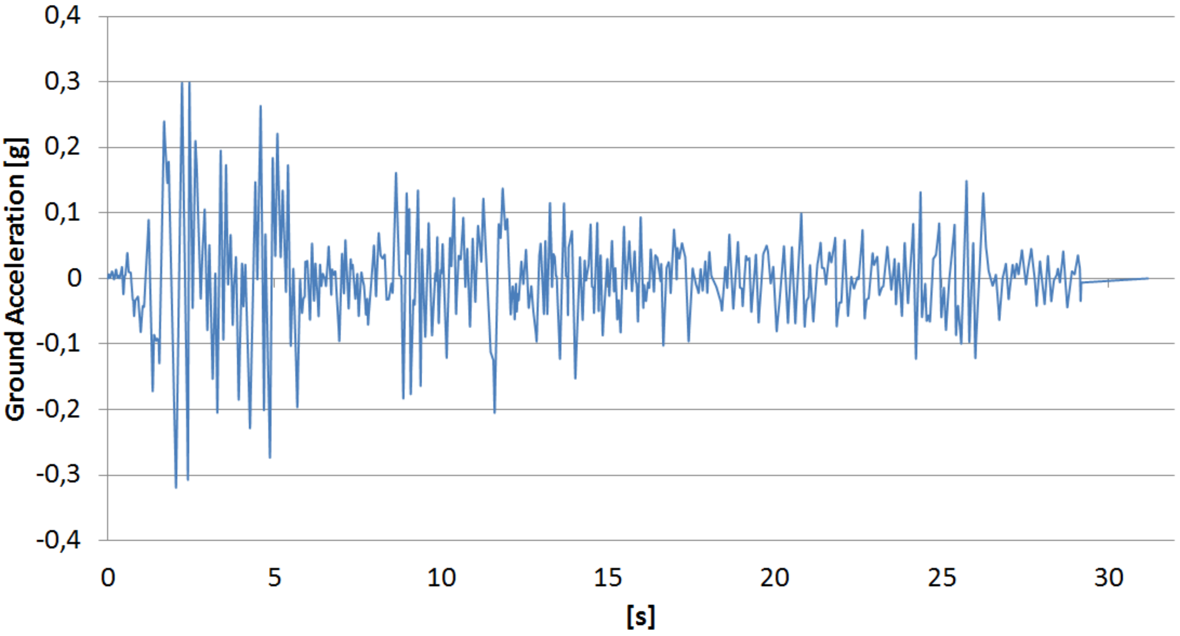

Figure 2.3: El Centro Ground Motion [4]

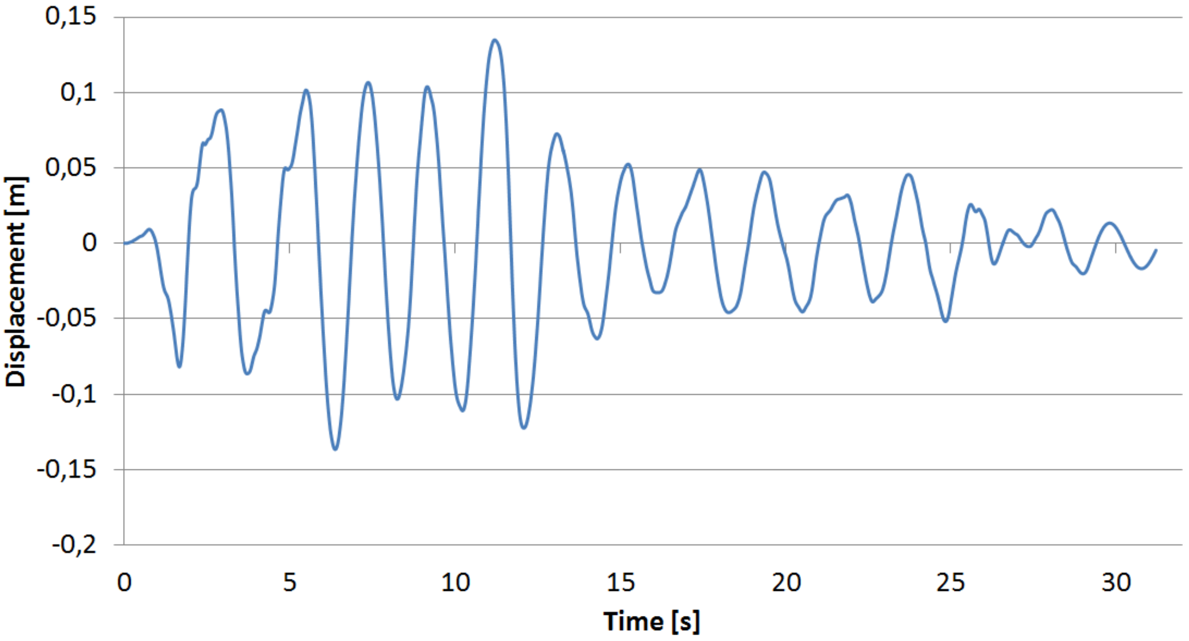

Figure 2.4: Displacement history

2.1.2 Hilber-Hughes-Taylor

Theory presented here is taken from Berkeley OpenSees Wiki [5] and the lecture notes by Mathisen [1]. Hilber-Hughes-Taylor is an implicit method that can handle numerical damping, without degrading the order of accuracy. This is convenient because introducing Rayleigh proportional damping in the Newmark methods mostly damps just the middle modes, and barely affects the higher and lower modes. To overcome these limitations, one can introduce algorithmic damping in the Newmark method by assigning γ with a value larger than 0.5. The problem with doing that, is a reduction of accuracy from $O(\Delta t^2)$ to $O(\Delta t)$.

In the Hilber-Hughes-Taylor-method the approximations of the Newmark method, shown in equations (2.1a) and (2.1b), are used. The time discrete momentum equation is then modified giving equation (2.25)

$$m\ddot{u}_{n+1} + (1+\alpha_H)c\dot{u}_{n+1} - \alpha_H c\dot{u}_n + (1+\alpha_H)ku_{n+1} - \alpha_H k d_n = R_\alpha^{ext} \tag{2.25}$$

When loads vary linearly over a time step the load vector may be written as seen in equation (2.26).

$$R_\alpha^{ext} = (1+\alpha_H)R_{n+1}^{ext} - \alpha_H R_n^{ext} \tag{2.26}$$

Hilber-Hughes-Taylor is more effective than Newmark to suppress high frequency noise, and decreasing the parameter α_H keeps th level of accuracy while increasing the amount of numerical dissipation.

In the following use of Hilber-Hughes-Taylor in SAP2000, α_H will be set to zero, practically making Hilbert-Hughes-Taylor equal to Newmarks average acceleration method. The reason for this choice is the lack of high frequency noise in the models, keeping the accuracy on a good level with the choice of $\alpha_H = 0$.

2.1.3 Non-linear Newmarks Method

The theory presented in this section is adapted from Chopra [3]. When doing non-linear time history direct integration, the non-linear Newmark method is a popular choice, and this subsection will present the underlying theory. When doing non-linear analysis the incremental equilibrium equation is as shown in equation (2.27)

$$m\Delta\ddot{u}_n + c\Delta\dot{u}_n + (\Delta f_S)_n = \Delta p_n \tag{2.27}$$

The incremental resisting force is

$$(\Delta f_S)_n = (k_n)_{sec}\Delta u_n \tag{2.28}$$

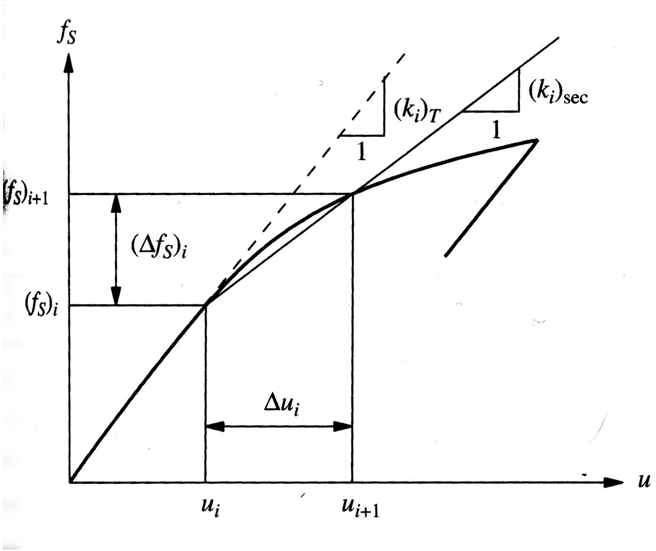

Figure 2.5: Illustration of secant and tangent stiffness [3]

$(k_n)_{sec}$ is the secant stiffness, illustrated in figure 2.5. This can not be determined due to the fact that u_{n+1} is not known. Because of this, the tangent stiffness, $(k_n)_T$ can be used instead. Putting it into equation (2.27) gives equation (2.29)

$$m\Delta\ddot{u}_n + c\Delta\dot{u}_n + (k_n)_T = \Delta p_n \tag{2.29}$$

This is similar to equation (2.21). The only change is the replacement of k with $(k_n)_T$ at each time step.

Using constant time steps can cause large errors for two main reasons

- Use of constant time steps delays the detection of transitions in the force-deformation relations
- Tangent Stiffness is used instead of secant stiffness

These errors are illustrated in figure 2.6, and can be reduced by using an iterative method. The important equation solved at each time step is

$$\hat{k}_T \Delta u = \hat{p} \tag{2.30}$$

Where

$$\hat{k}_T = (k_n)_T + \frac{\gamma}{\beta\Delta t}c + \frac{1}{\beta(\Delta t)^2} \tag{2.31}$$

The non-linear stiffness is not constant. Equation (2.30) is shown in figure 2.7, and the iterative procedure illustrated is described in more detail here: The first step is to determine $u^{(1)}$ by using equation (2.30). The force $\Delta f^{(1)}$ which is connected to $u^{(1)}$ is less than $\Delta\hat{p}$ and the residual force becomes $\Delta R^{(2)} = \Delta\hat{p} - \Delta f^{(1)}$. Additional displacement $\Delta u^{(2)}$ from $\Delta R^{(2)}$ is found by

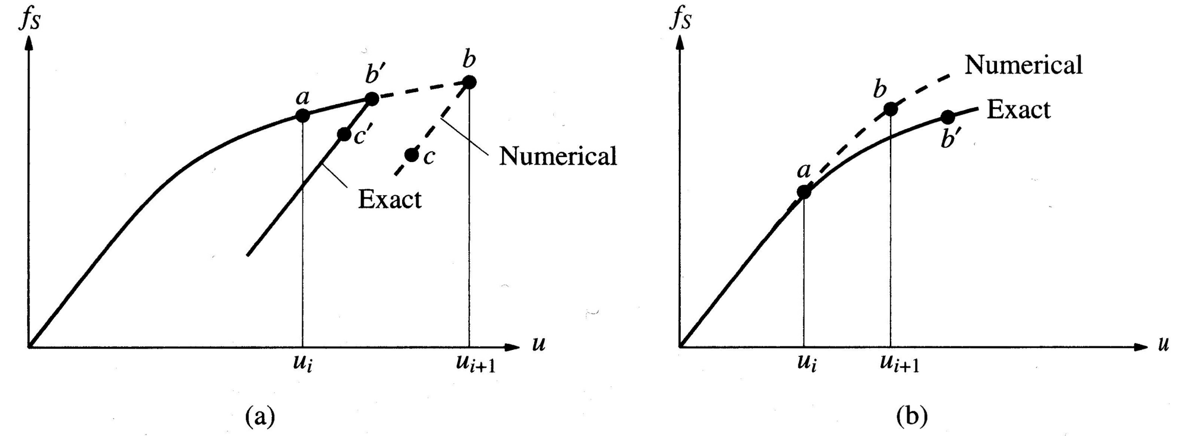
fS
a
b′
b
c′
c
Numerical
Exact
u
u_i
u_{i+1}
(a)
fS
Numerical
b
Exact
b′
a
u
u_i
u_{i+1}
(b)

Figure 2.6: Illustration of numerical errors [3]

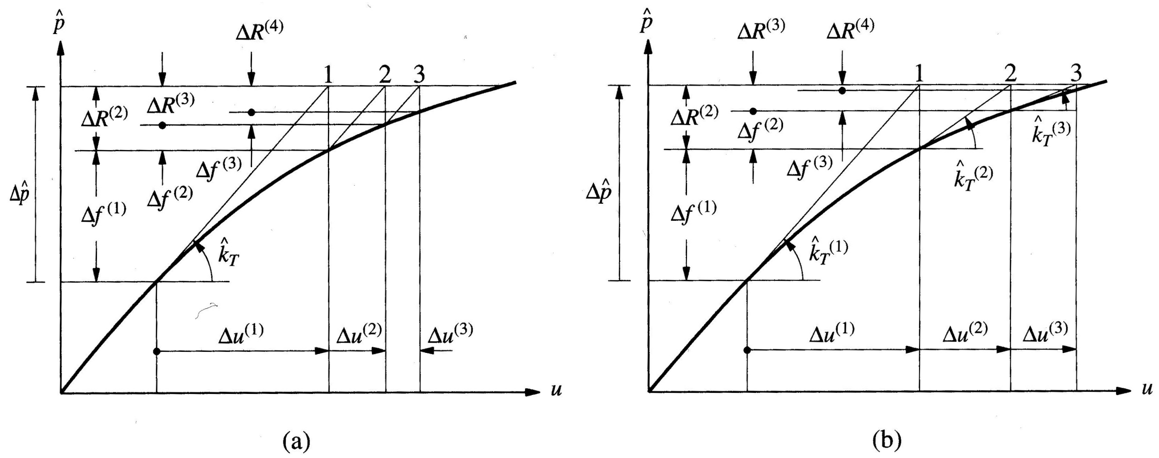
p̂
ΔR(4)
1
2
3
ΔR(2)
ΔR(3)
Δf(3)
Δp̂
Δf(1)
Δf(2)
k̂T
Δu(1)
Δu(2)
Δu(3)
u
(a)
p̂
ΔR(3)
ΔR(4)
1
2
3
ΔR(2)
Δf(2)
k̂T(3)
Δp̂
Δf(3)
k̂T(2)
Δf(1)
k̂T(1)
Δu(1)
Δu(2)
Δu(3)
u
(b)

Figure 2.7: Illustration of iterations [3]

$$\hat{k}_T \Delta u^{(2)} = \Delta R^{(2)} = \Delta \hat{p} - \Delta f^{(1)} \tag{2.32}$$

This displacement is used to find a new magnitude of the residual force, and repeated until it converges. This iterative process is listed below

1. Initialize data
    (a) $u_{n+1}^{(0)} = u_n \quad f_S^{(0)} = (f_S)_n \quad \Delta R^{(1)} = \Delta \hat{p}_n \quad \hat{k}_T = \hat{k}_n$
2. Calculations for each iteration
    (a) Solve $\hat{k}_T \Delta u^{(j)} = \Delta R^{(j)} \to \Delta u^{(j)}$
    (b) $u_{n+1}^{(j)} = u_{n+1}^{(j-1)} + \Delta u^{(j)}$
    (c) $\Delta f^{(j)} = f_S^{(j)} - f_S^{(j-1)} + (\hat{k}_T - k_T)\Delta u^{(j)}$
    (d) $\Delta^{(j+1)} = \Delta R^{(j)} - \Delta f^{(j)}$
3. Repeat for next iteration, replace j with $j+1$

The iterations are repeated until the incremental displacement $\Delta u^{(l)}$ becomes small enough in comparison to the current estimate of Δu.

$$\frac{\Delta u^{(l)}}{\sum\limits_{j=1}^{l} \Delta u^{(j)}} < \varepsilon \tag{2.33}$$

When Δu_n is found, the process continues as shown in section 2.1.1, except that

$$\ddot{u}_{n+1} = \frac{p_{n+1} - c\dot{u}_{n+1} - ku_{n+1}}{m} \tag{2.34}$$

2.2 Numerical Damping

The information in this section is obtained from CSI Berkeley's online wiki [6]. The damping used by SAP2000 for direct integration time history analysis is called mass- and stiffness-proportional damping. Another word for this damping is Rayleigh Damping, and it is commonly used when running non-linear dynamic analysis. When formulated, the damping matrix is said to be proportional to the stiffness and mass matrix as shown in equation (2.35)

$$c = \eta m + \delta k \tag{2.35}$$

The mass proportional damping coefficient is η and the stiffness damping coefficient is δ. They are related through orthogonality and modal equation as follows in equation (2.36)

$$\zeta_n = \frac{1}{2\omega_n}\eta + \frac{\omega_n}{2}\delta \tag{2.36}$$

ζ_n is the critical damping ratio, and ω_n is the natural frequency of the system. This shows that the damping ratio is not constant with the natural frequency. The variables η and δ are given at two frequencies where the damping is known, or assumed. The critical damping ratio will then be smaller between the two frequencies chosen, and larger outside.

In SAP2000 the coefficients η and δ can be designated directly, or a given critical damping ratio can be given at two different frequencies or periods. If the critical damping for two periods or frequencies are set equal, the proportionality factors simplify as shown in equation (2.37).

$$\zeta_i = \zeta_j = \zeta \text{ hence } \delta = \frac{2\zeta}{\omega_i + \omega_j} \text{ and } \eta = \omega_i \omega_j \delta \tag{2.37}$$

Chapter 3

Elastic Analysis

This chapter will present the basic theory on which modal analysis of elastic buildings are based on. A calculation using this theory will be performed, and compared with a similar analysis done with the program SAP2000. The theory is adapted from Tam Larkin [2], Nawawi Chouw [7] and Chopra [3]

3.1 Symmetric Plan Buildings

3.1.1 Modal Analysis

The equations of motion for a MDOF-system are

$$\mathbf{m}\ddot{\mathbf{u}} + \mathbf{c}\dot{\mathbf{u}} + \mathbf{k}\mathbf{u} = \mathbf{p}(t) \tag{3.1}$$

For an undamped system, the modes are uncoupled. This is not always correct if the system has damping, but for some types that are justifiable idealizations for many structures, uncoupled damping can be used as well. The dynamic response of a system can then be expressed as equation (3.2)

$$\mathbf{u}(t) = \sum_{r=1}^{N} \phi_r q_r(t) = \mathbf{\Phi}\mathbf{q}(t) \tag{3.2}$$

If equation (3.2) is substituted into equation (3.1), equation (3.3) is obtained

$$\sum_{r=1}^{N} \mathbf{m}\phi_r \ddot{q}_r(t) + \sum_{r=1}^{N} \mathbf{c}\phi_r \dot{q}_r(t) + \sum_{r=1}^{N} \mathbf{k}\phi_r q_r(t) = \mathbf{p}(t) \tag{3.3}$$

To use the orthogonality properties of modes, all of terms are pre-multiplied by ϕ_n^T

$$\sum_{r=1}^{N} \phi_n^T \mathbf{m}\phi_r \ddot{q}_r(t) + \sum_{r=1}^{N} \phi_n^T \mathbf{c}\phi_r \dot{q}_r(t) + \sum_{r=1}^{N} \phi_n^T \mathbf{k}\phi_r q_r(t) = \phi_n^t \mathbf{p}(t) \tag{3.4}$$

Orthogonality causes all terms of the summation, except r=n, to disappear, reducing equation (3.4) to

$$(\phi_n^T \mathbf{m} \phi_n)\ddot{q}_n(t) + (\phi_n^T \mathbf{c} \phi_n)\dot{q}(t) + (\phi_n^T \mathbf{k} \phi_n) q_n(t) = \phi_n^T \mathbf{p}(t) \tag{3.5}$$

The following notation is then adapted

$$M_n = \phi_n^T \mathbf{m} \phi_n \quad C_n = \phi_n^T \mathbf{c} \phi_n \quad K_n = \phi_n^T \mathbf{k} \phi_n \quad P_n(t) = \phi_n^T \mathbf{p}(t) \tag{3.6}$$

Using this and classical damping, equation (3.5) can be written like this

$$M_n \ddot{q}_n(t) + C_n \dot{q}_n(t) + K_n q_n(t) = P_n(t) \tag{3.7}$$

This equation exists for all N modes, and can be written on matrix form:

$$\mathbf{M}\ddot{\mathbf{q}} + \mathbf{C}\dot{\mathbf{q}} + \mathbf{K}\mathbf{q} = \mathbf{P}(t) \tag{3.8}$$

This is used to solve N SDOF systems with the parameters M_n, K_n, C_n and P_n, and combining them gives the total response. Dividing equation (3.7) by M_n renders

$$\ddot{q}_n + 2\zeta_n \omega_n \dot{q}_n + \omega_n^2 q_n = \frac{P_n(t)}{M_n} \tag{3.9}$$

Here ζ_n is the damping ratio for the nth mode.

When each of the SDOF systems are solved, the contribution to nodal displacement $\mathbf{u}_n(t)$ from mode n is given by this

$$\mathbf{u}_n(t) = \phi_n q_n(t) \tag{3.10}$$

And combining all the modal contributions to find total displacements

$$\mathbf{u}(t) = \sum_{n=1}^{N} \mathbf{u}_n(t) = \sum_{n=1}^{N} \phi_n q_n(t) \tag{3.11}$$

This procedure has many names, for example classical modal analysis, classical mode superposition method, or more precisely classical mode displacement superposition method. Its short name is just modal analysis, and it is restricted only to linear system. This because superposition can only be used in a linear systems. The damping also has to be of the classical form to obtain uncoupled modal equations.

The procedure to solve the dynamic response of a MDOF system can be summarized like Chopra [3] has done:

1. Define structural properties
    (a) Determine the stiffness matrix **k** and mass matrix **m**
    (b) Estimate modal damping ratios ζ_n

2. Calculate the natural frequencies ω_n and modes ϕ_n
3. Compute the response in each mode by the following steps
   (a) Set up equation (3.7) and solve for $q_n(t)$
   (b) Compute nodal displacement $\mathbf{u}_n(t)$ from equation (3.10)
   (c) Compute element forces associated with the nodal displacements
4. Combine the contributions of all the modes to determine the total response, using equation (3.11)

3.1.2 Modal Response Contributions

Modal Expansion of Excitation Vector

The expansion of the excitation vector is useful because of two main reasons

- $\mathbf{s}_n p(t)$ only produces response in the nth mode, and no response in any other mode
- The dynamic response in the nth mode is due entirely to the partial force vector $\mathbf{s}_n p(t)$

To expand the vector $\mathbf{p}(t)$, it is divided into a time variation part, $p(t)$, and a spatial distribution part $\mathbf{s}$

$$\mathbf{p}(t) = \mathbf{s}p(t)$$

It can be helpful to expand $\mathbf{s}$ like this

$$\mathbf{s} = \sum_{r=1}^{N} \mathbf{s}_r = \sum_{r=1}^{N} \Gamma_r \mathbf{m} \phi_r \tag{3.12}$$

Pre-multiplying this equation with ϕ_n^T and using the orthogonal properties of modes gives

$$\Gamma_n = \frac{\phi_n^T \mathbf{s}}{M_n} \tag{3.13}$$

This gives the contribution of the nth mode to $\mathbf{s}$

$$\mathbf{s}_n = \Gamma_n \mathbf{m} \phi_n \tag{3.14}$$

Equation (3.12) can also be viewed as an expansion of the distribution $\mathbf{s}$ of applied forces in terms of inertia force distribution $\mathbf{s}_n$ associated with natural modes. This interpretation can be observed by considering the structure vibrating in its nth mode with accelerations $\ddot{\mathbf{u}}(t) = \ddot{q}_n(t)\phi_n$. The associated inertia forces are

$$(\mathbf{f}_I)_n = -\mathbf{m}\ddot{\mathbf{u}}_n(t) = -\mathbf{m}\phi_n \ddot{q}_n(t) \tag{3.15}$$

Their spatial distribution $\mathbf{m}\phi_n$ is the same as that of $\mathbf{s}_n$ To use this for dynamic analysis the generalized force $P_n(t) = \Gamma M_n p(t)$ for the nth mode is substituted into equation (3.9) to obtain the modal equation

$$\ddot{q}_n + 2\zeta_n\omega_n\dot{q}_n + \omega_n^2 q_n = \Gamma_n p(t) \tag{3.16}$$

The solution of $q_n(t)$ can be written in terms of the response of a SDOF system with $m = 1$ and $\zeta = \zeta_n$. For this special case we use D instead of q.

$$\ddot{D}_n + 2\zeta_n\omega_n\dot{D}_n + \omega_n^2 D_n = p(t) \tag{3.17}$$

Comparing equation (3.16) and (3.17) it seen that

$$q_n(t) = \Gamma_n D_n(t) \tag{3.18}$$

This shows that $q_n(t)$ is easily obtainable when equation (3.17) has been solved for $D_n(t)$, utilizing regular SDOF solution methods. The contribution to the nodal displacement $\mathbf{u}(t)$ from the nth mode is then

$$\mathbf{u}_n(t) = \Gamma_n\phi_n D_n(t) \tag{3.19}$$

And the equivalent static forces become

$$\mathbf{f}_n(t) = \mathbf{s}_n[\omega_n^2 D_n(t)] \tag{3.20}$$

The nth mode contribution to $r_n(t)$ to any response quantity $r(t)$ is determined by static analysis of the structure subjected to forces $\mathbf{f}_n(t)$. The static value of r due to external forces $\mathbf{s}_n$ is noted as r_n^{st} giving the following expression

$$r_n(t) = r_n^{st}[\omega_n^2 D_n(t)] \tag{3.21}$$

When all the modes are combined, the total response is given as

$$r(t) = \sum_{n=1}^{N} r_n(t) = \sum_{n=1}^{N} r_n^{st}[\omega_n^2 D_n(t)] \tag{3.22}$$

This means that the contribution of $r_n(t)$ of the nth mode to the dynamic response is the product of two analyses. First the static analysis of the structure excited by the external force $\mathbf{s}_n$ and secondly the dynamic analysis of the nth mode SDOF system excited by the force $p(t)$, as is shown schematically in figure 3.1

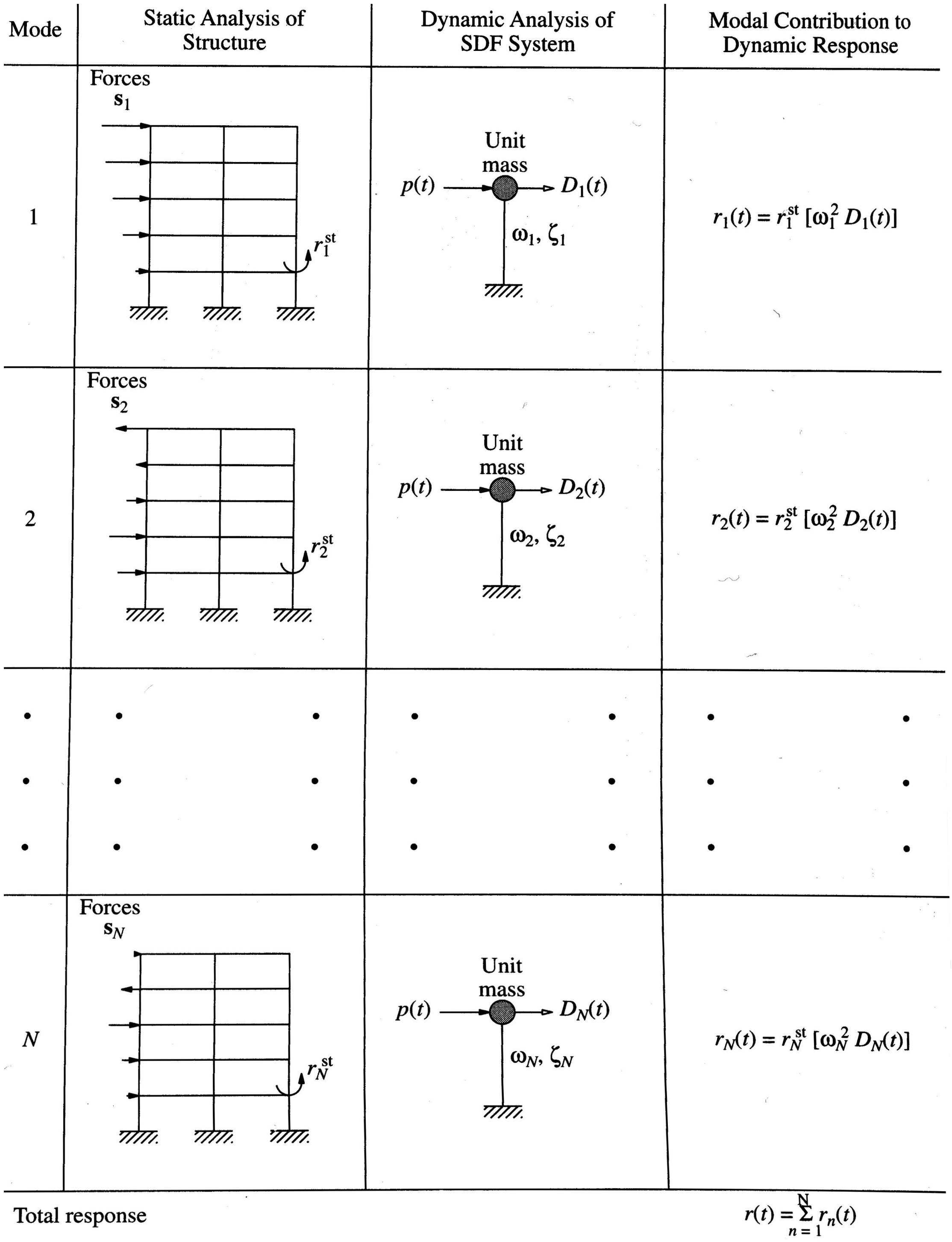
Mode
Static Analysis of Structure
Dynamic Analysis of SDF System
Modal Contribution to Dynamic Response
1
Forces $\mathbf{s}_1$
r_1^{st}
Unit mass
$p(t)$
$D_1(t)$
ω_1, ζ_1
$r_1(t) = r_1^{st}\,[\omega_1^2 D_1(t)]$
2
Forces $\mathbf{s}_2$
r_2^{st}
Unit mass
$p(t)$
$D_2(t)$
ω_2, ζ_2
$r_2(t) = r_2^{st}\,[\omega_2^2 D_2(t)]$
N
Forces $\mathbf{s}_N$
r_N^{st}
Unit mass
$p(t)$
$D_N(t)$
ω_N, ζ_N
$r_N(t) = r_N^{st}\,[\omega_N^2 D_N(t)]$
Total response
$r(t) = \sum_{n=1}^{N} r_n(t)$

Figure 3.1: Schematic description of modal response [3]

Modal Contribution Factors

Equation (3.21) can be expressed as

$$r_n(t) = r^{st}\bar{r}_n[\omega_n^2 D_n(t)] \tag{3.23}$$

where $\bar{r}_n$ is the static value of r due to external forces $\mathbf{s}$, an the nth modal contribution factor

$$\bar{r}_n = \frac{r_n^{st}}{r^{st}} \tag{3.24}$$

These modal contribution factors $\bar{r}_n$ have three important properties

- They are dimensionless
- They are independent of how the modes are normalized
- The sum of the modal contribution factors over all modes is unity, $\sum\limits_{n=1}^{N} \bar{r}_n = 1$

Modal Combination Rules

This part has been adapted from my project from the fall of 2011.

The peak modal response r_{no} for mode n is found like this $r_{no} = r_n^{st} A_n$, where r_n^{st} is the modal static response, and A_n is the pseudo acceleration ordinate $A(T_n, \zeta_n)$. It is not possible to find the exact value of r_o from the modal responses, because their maximum does not occur at the same time. If all the maximum modal responses are added together, $r_o = \sum\limits_{n=1}^{N} |r_{no}|$, an upper bound value will be acquired, and this is usually very conservative. This happens because there is a very low probability for all modal maximums to happen at the same time.

To get around this problem E. Rosenblueth in 1951 developed the square-root-of-sum-of-squares (SRSS) rule for modal combination. It states that the peak response for each mode is squared, summed and then taken the square root of: $r_o \simeq \sqrt{\sum\limits_{n=1}^{N} r_{no}^2}$. This provides very good estimates, but has a limitation when the modes natural periods are close. Another method is then used to avoid this problem. It is named the complete quadratic combination (CQC), and it is formulated like this $r_o \simeq \sqrt{\sum\limits_{i=1}^{N} \sum\limits_{n=1}^{N} \rho_{in} r_{io} r_{no}}$. ρ_{in} varies from 0 to 1 when $i = n$. It can also be written as follows to show that the first summation is identical to the SRSS rule. The CQC can turn out both larger and smaller than SRSS.

$$r_o \simeq \sum_{n=1}^{N} r_{no}^2 + \underbrace{\sum_{i=1}^{N} \sum_{n=1}^{N}}_{i \neq n} \rho_{in} r_{io} r_{no}$$

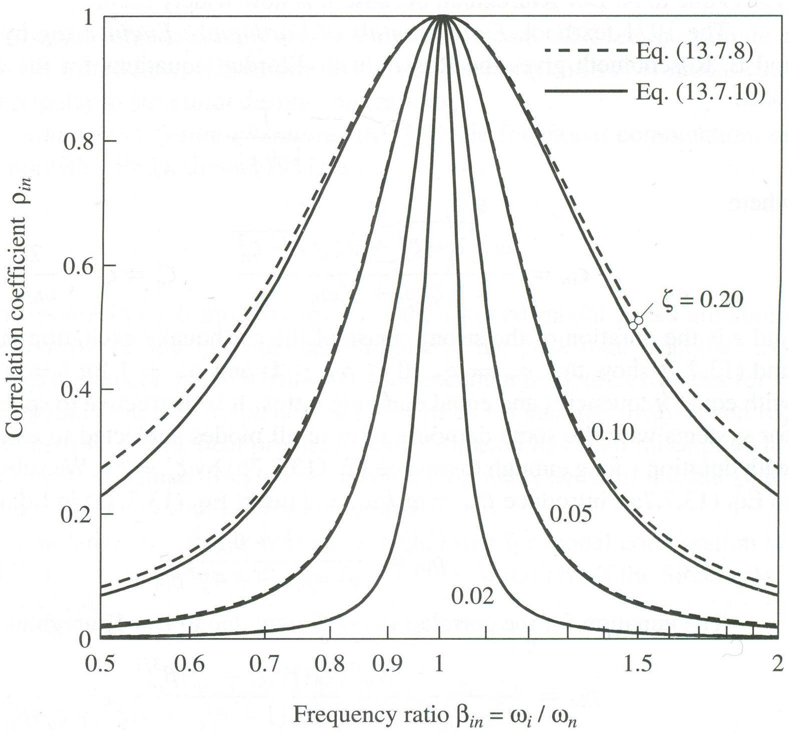

Figure 3.2: Correlation Factor [3]

There are also several formulations for the correlation coefficient ρ_{in}, and the most used one now, according to Chopra is the one found by A. Der Kiureghian in 1981. It is, for equal modal damping like this:

$$\rho_{in} = \frac{8\zeta^2(1+\beta_{in})\beta_{in}^{\frac{3}{2}}}{(1-\beta_{in}^2)^2 + 4\zeta^2\beta_{in}(1+\beta_{in}^2)^2} \tag{3.25}$$

Where ζ is the damping ratio and $\beta_{in} = \frac{\omega_i}{\omega_n}$. Figure 3.2 shows how ρ_{in} varies with β_{in}, and how it gets large if there is close modal periods. In a 5% damped structure $\rho_{in} > 0,1$ only when $\frac{1}{1{,}35} \leq \beta_{in} \leq 1,13$. This shows how CQC turns in to SRSS if the modal periods are wide enough apart.

Both SRSS and CQC are derived from random vibration theory, and are therefore most accurate for loading with a wide frequency content and long phases of strong shaking. It is less accurate for short impulsive loads or for many cycles of harmonic excitations. These methods are best used with smooth response spectra based, and they tend to have errors on the non-conservative side. This means that the response spectrum has to be on the conservative side. Errors up to 25% have been observed for local response quantities.

3.1.3 Response Spectrum Analysis Procedure

There are two main ways to do earthquake analysis of linear systems. Namely Response History Analysis (RHA) and Response Spectrum Analysis (RSA). RHA is a more labour-intensive analysis because it provides a structural response $r(t)$ as a function of time over the duration of a shaking event. For a SDOF RSA will provide the same result, but that is not the case for a MDOF-situation. But it does provide a good estimate.

For a N-story building with a plan symmetric about two axes, you can compute the peak response as follows from Chopra [3]:

1. Define the structural properties
   (a) Determine the mass matrix $\mathbf{m}$ and the lateral stiffness matrix $\mathbf{k}$
   (b) Estimate the modal damping ratios ζ_n
2. Determine the natural frequencies ω_n and natural modes ϕ_n of vibration
3. Compute the peak response in the nth mode
   (a) Corresponding to natural period T_n and damping ratio ζ_n, read D_n and A_n from the response or design spectrum
   (b) Compute the floor displacement and story drifts with $u_{jn} = \Gamma_n \phi_{jn} D_n$ and $\Delta_{jn} = \Gamma_n(\phi_{jn} - \phi_{j-1,n})D_n$
   (c) Compute equivalent static forces $\mathbf{f}_n$ from $f_{jn} = \Gamma_n m_j \phi_{jn} A_n$
   (d) Compute the story forces, shear and overturning moment, and element forces, bending moments and shear, by static analysis of the structure subjected to lateral forces $\mathbf{f}_n$.
4. Determine an estimate for the peak value r of any response quantity by combining the peak modal values r_n according to SRSS or CQC depending on the spacing of the modal frequencies.

When using this method it is important to be aware that it is wrong to compute the combined peak value of a response quantity from the combined peak values of other response quantities. The correct procedure is to combine the peak modal values, and then calculating the combined peak of this.

3.1.4 Elastic Analysis of a 2D-frame

In this section a double bay, five story shear frame will be analysed by the use of an elastic modal response spectrum analysis. The structure consists of HE120A beams and columns and is simplified to work as a shear structure. The model is shown in figure 3.3. Each bay is 6 meters wide, and each story is 3 meters high.

The system has the following K-matrix:

$$K = \begin{bmatrix} 3\,393\,600 & -1\,696\,800 & 0 & 0 & \\ -1\,696\,800 & 3\,393\,600 & -1\,696\,800 & 0 & 0 \\ 0 & -1\,696\,800 & 3\,393\,600 & -1\,696\,800 & 0 \\ 0 & 0 & -1\,696\,800 & 3\,393\,600 & -1\,696\,800 \\ 0 & 0 & 0 & -1\,696\,800 & 1\,696\,800 \end{bmatrix} [\text{N/m}] \qquad (3.26)$$

The mass of the frame is put as distributed loads on each floor equal to 5 kN/m, giving the

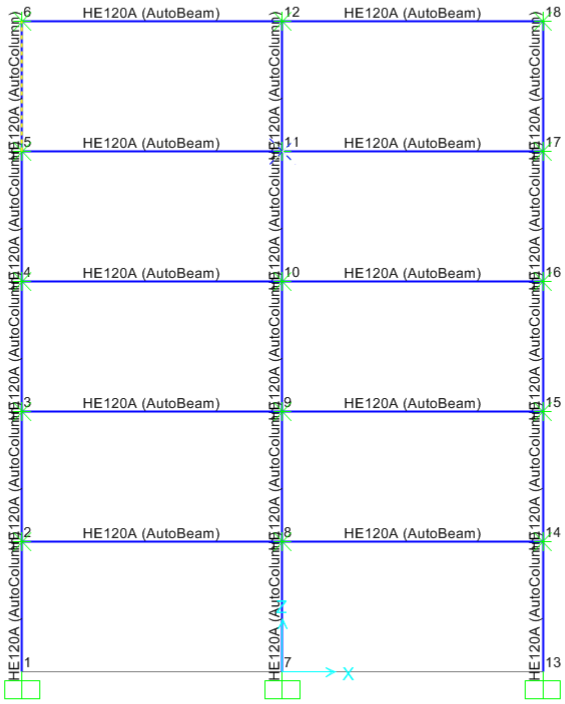
6
HE120A (AutoBeam)
12
HE120A (AutoBeam)
18
5
HE120A (AutoBeam)
11
HE120A (AutoBeam)
17
4
HE120A (AutoBeam)
10
HE120A (AutoBeam)
16
3
HE120A (AutoBeam)
9
HE120A (AutoBeam)
15
2
HE120A (AutoBeam)
8
HE120A (AutoBeam)
14
1
7
13
HE120A (AutoColumn)
Z
X

Figure 3.3: Multi-story Frame

following mass matrix

$$M = \begin{bmatrix} 6116.2 & 0 & 0 & 0 & 0 \\ 0 & 6116.2 & 0 & 0 & 0 \\ 0 & 0 & 6116.2 & 0 & 0 \\ 0 & 0 & 0 & 6116.2 & 0 \\ 0 & 0 & 0 & 0 & 6116.2 \end{bmatrix} [\mathrm{kg}] \tag{3.27}$$

Solving the eigenvalue problem gives following periods

$$\begin{bmatrix} 1.3253 \\ 0.4540 \\ 0.2880 \\ 0.2242 \\ 0.1966 \end{bmatrix} [\mathrm{s}] \tag{3.28}$$

And the normalized mode shapes shown in figure 3.4

The modal participation factors are found by

$$\Gamma_n = \frac{\boldsymbol{\phi}_n^T \mathbf{m} \boldsymbol{\iota}}{\boldsymbol{\phi}_n^T \mathbf{m} \boldsymbol{\phi}_n} \tag{3.29}$$

Giving

$$\Gamma = \begin{bmatrix} 1.2517 \\ -0.3621 \\ 0.1586 \\ -0.0632 \\ 0.0150 \end{bmatrix} \tag{3.30}$$

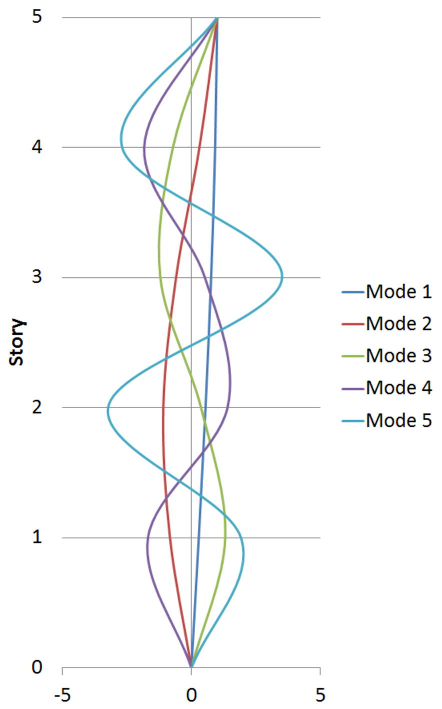

Figure 3.4: Normalized mode shapes

At this point the information needed to perform a modal analysis is found. In this example the pseudo acceleration response spectrum from El Centro will be used to calculate the different responses. The ground motion and spectrum is included in figure 2.3 and 3.5, respectively.

Accelerations are found from the spectrum, and spectral displacements are found by

$$D_n = \frac{S_{an}}{\omega_n^2}$$

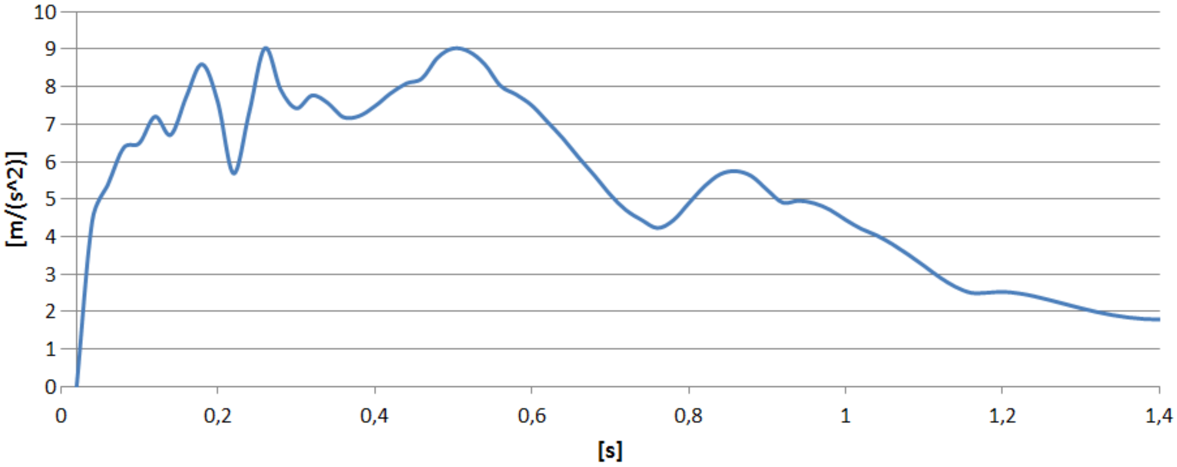

Figure 3.5: Response spectrum for El Centro ground motion for 5% damping

Giving

$$S_a = \begin{bmatrix} 1.99 \\ 8.10 \\ 7.70 \\ 5.60 \\ 7.59 \end{bmatrix} \left[\frac{\mathrm{m}}{\mathrm{s}^2}\right] \qquad S_d = \begin{bmatrix} 0.0866 \\ 0.0423 \\ 0.0162 \\ 0.0071 \\ 0.0074 \end{bmatrix} [\mathrm{m}] \tag{3.31}$$

The modal story displacements are then found by

$$\mathbf{u} = \boldsymbol{\Gamma\phi}\mathbf{S_d} \tag{3.32}$$

Giving

$$u = \begin{bmatrix} 0.0316 & 0.0127 & 0.0034 & 0.0008 & 0.0002 \\ 0.0606 & 0.0167 & 0.0010 & -0.0006 & -0.0004 \\ 0.0847 & 0.0091 & -0.0031 & -0.0002 & 0.0004 \\ 0.1020 & -0.0047 & -0.0018 & 0.0008 & -0.0003 \\ 0.1109 & -0.0153 & 0.0025 & -0.0005 & 0.0001 \end{bmatrix} [\mathrm{m}] \tag{3.33}$$

Combined with SRSS the floor displacements are estimated as

$$u_{srss} = \begin{bmatrix} 0.0342 \\ 0.0629 \\ 0.0852 \\ 0.1021 \\ 0.1120 \end{bmatrix} [\mathrm{m}] \tag{3.34}$$

Similar calculations are done for base shear providing the following result

$$V_b = \begin{bmatrix} 53.5 \\ 21.6 \\ 5.70 \\ 1.29 \\ 0.36 \end{bmatrix} [\mathrm{kN}] \qquad V_{srss} = \sum_{n=1}^{N} \sqrt{V_{bn}^2} = 58.06\mathrm{kN} \tag{3.35}$$

SAP2000 Calculations

The structure has also been analysed in SAP2000 for a more accurate solution of the problem. This is important because the simplification of a shear building with no bending of the beams is unrealistic.

The Model SAP2000 has calculated the response via several methods that will be compared with the hand calculation. These include response spectrum, linear modal history and linear direct integration history. The model is fixed to the ground and consists of the same HE120A beams and columns as said in the beginning of section 3.1.4. The mass is implemented as a distributed 5 kN/m load on each floor. Plastic hinges are assigned, but will not be affecting the results in this section due to the linearity of the analysis performed here. All joints are restrained for movement in the y-direction, out of the plane . The bays are still 6 meters wide, and stories 3 meters high. The load will be applied as a response spectrum, linear modal history and linear direct integration history. The ground motion and response spectrum applied are shown in figure 2.3 and 3.5, respectively.

- Linear modal history used the method of modal superposition and solves it for each time step, modal damping is kept fixed at 0.05. The time step will be 0.02 seconds, same as the ground motion record, and to cover the 30 second long ground motion 1500 time steps have been chosen.
- Linear direct integration solves the whole structure for each time step. The time step will be 0.02 seconds, same as the ground motion record, and to cover the 30 second long ground motion 1500 time steps have been chosen. It has proportional damping specified by period that gives a mass proportional coefficient of 0.5984 and a stiffness proportional coefficient of $7.599 * 10^{-4}$ when the damping ratio is 0.05. The time integration is done by Hilber-Hughes-Taylor with standard coefficients of Gamma=0.5, Beta=0.25 and Alpha=0.
- Response spectrum finds the maximum response for each mode and combines it with SRSS. 0.05 damping is also used here. (see section 3.1.2)

Table 3.1 compares the period of the modes of the SAP2000-model, and the hand calculated one.

Table 3.1: Comparison of modal periods

Mode	Shear building	SAP2000 Model
1	1.3253 sec	2.4937 sec
2	0.4540 sec	0.7801 sec
3	0.2880 sec	0.4247 sec
4	0.2242 sec	0.2801 sec
5	0.1966 sec	0.2166 sec

The difference between the two result are because a shear structure assumes that the stories does not deform, making the system stiffer, hence reducing the period. The model in SAP2000 does include the stiffness of the beams hence softening the system. The modes does have the same shape in each instance.

In table 3.2 maximum base shear and roof displacement are compared

Table 3.2: Comparison of base shear and roof displacement

Case	Base shear	Roof Displacement
Shear Structure	58.06 kN (Eq (3.35))	0.1120 m (Eq (3.34))
Linear Modal History	51.35 kN	0.3684 m
Linear Direct Integration	52.63 kN	0.3774 m
Response Spectrum	50.96 kN	0.3534 m

The increased stiffness has a low impact on the base shear. This makes sense since the mass accelerated by the quake is the same in all systems. This is not valid for the roof

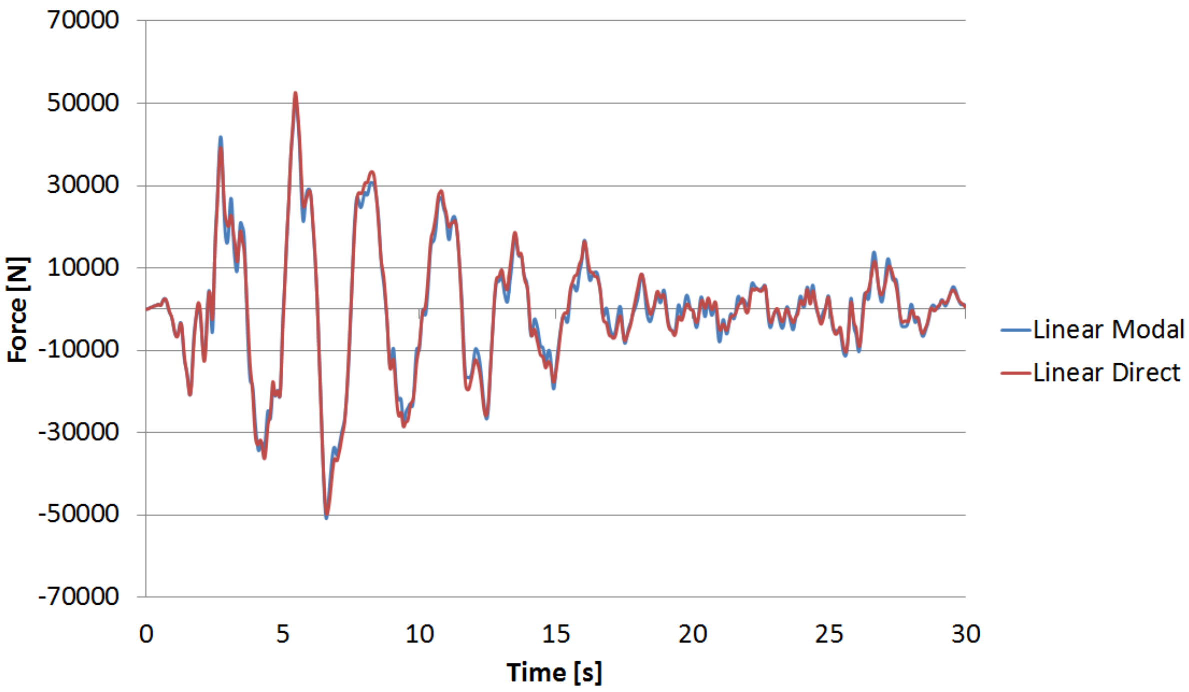

Figure 3.6: Comparison of time history of base shear for Linear Modal History and Linear Direct Integration

displacement. Here the difference in stiffness causes a large difference between the shear story model and the SAP2000 model. This is to be expected. The difference between Linear Modal History and Linear Direct integration is caused by the way damping is implemented in the two cases. This causes a small deviation. The difference between response spectrum and the two others comes from the resolution of the response spectrum.

Figure 3.6 shows the time history of the base shear for the Linear Modal History and the Linear Direct Integration.

The time history verifies what was shown in table 3.2 occurs over the whole time history.

This section has shown that there are several shortcomings when you model a structure as a shear building. Using linear analysis the computational power demanded by the different analysis is quite low no matter which one is chosen, and hence the accurate direct integration can be used just as well as linear modal history. The problem with using time histories is that several relevant time histories has to be analysed, since no quake is the same. This is where the response spectrum method has its advantage, since a design spectrum can easily be implemented.

3.2 Asymmetric Plan Buildings

This section will present the theory behind linear analysis of asymmetric plan buildings. First a one story system will be described, then a multi-story system. In the end a SAP2000 analysis of a steel moment resisting frame structure with asymmetric plan will be analysed using response spectrum analysis with both CQC and SRSS to compare the effect of the modal combination factor.

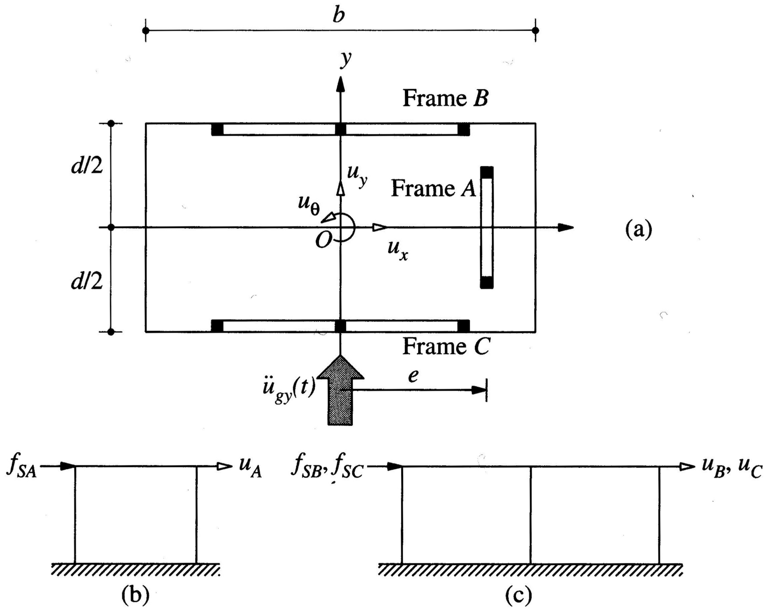

Figure 3.7: Illustration of asymmetric system

3.2.1 One Story, Two Way Asymmetric System

The system and theory from Chopra [3] will be presented here. The system is a one story building consisting of three frames, A,B and C and a roof diaphragm that is rigid in its own plane. Figure 3.7 illustrates the system. Frame B and C are oriented in the x-direction while Frame A is oriented in the y-direction.

The force displacement relation can be expressed as follows

$$\begin{bmatrix} f_{Sx} \\ f_{Sy} \\ f_{S\theta} \end{bmatrix} = \begin{bmatrix} k_{xx} & k_{xy} & k_{x\theta} \\ k_{yx} & k_{yy} & k_{y\theta} \\ k_{\theta x} & k_{\theta y} & k_{\theta\theta} \end{bmatrix} \begin{bmatrix} u_x \\ u_y \\ u_\theta \end{bmatrix} \quad \text{or} \quad \mathbf{f}_S = \mathbf{k}\mathbf{u} \tag{3.36}$$

The elements in the stiffness matrix **k** can be determined by the direct equilibrium method. The lateral stiffness of each frame is defined as follows

$$f_{SA} = k_y u_A \quad f_{SB} = k_{xB} u_B \quad f_{SC} = k_{xC} u_C \tag{3.37}$$

By imposing unit displacements for each DOF successively as shown in figure 3.8 the following **k** is acquired

$$\mathbf{k} = \begin{bmatrix} k_{xB} + k_{xC} & 0 & (d/2)(k_{xC} - k_{xB}) \\ 0 & k_y & ek_y \\ (d/2)(k_{xC} - k_{xB}) & ek_y & e^2 k_y + (d^2/4)(k_{xB} + k_{xC}) \end{bmatrix} \tag{3.38}$$

Direct stiffness method could also be used to acquire this matrix. The inertia forces on the mass components are, since the DOFs are located at centre of mass O, as follows

$$f_{Ix} = m\ddot{u}_x^t \quad f_{Iy} = m\ddot{u}_y^t \quad f_{I\theta} = I_O \ddot{u}_\theta^t \tag{3.39}$$

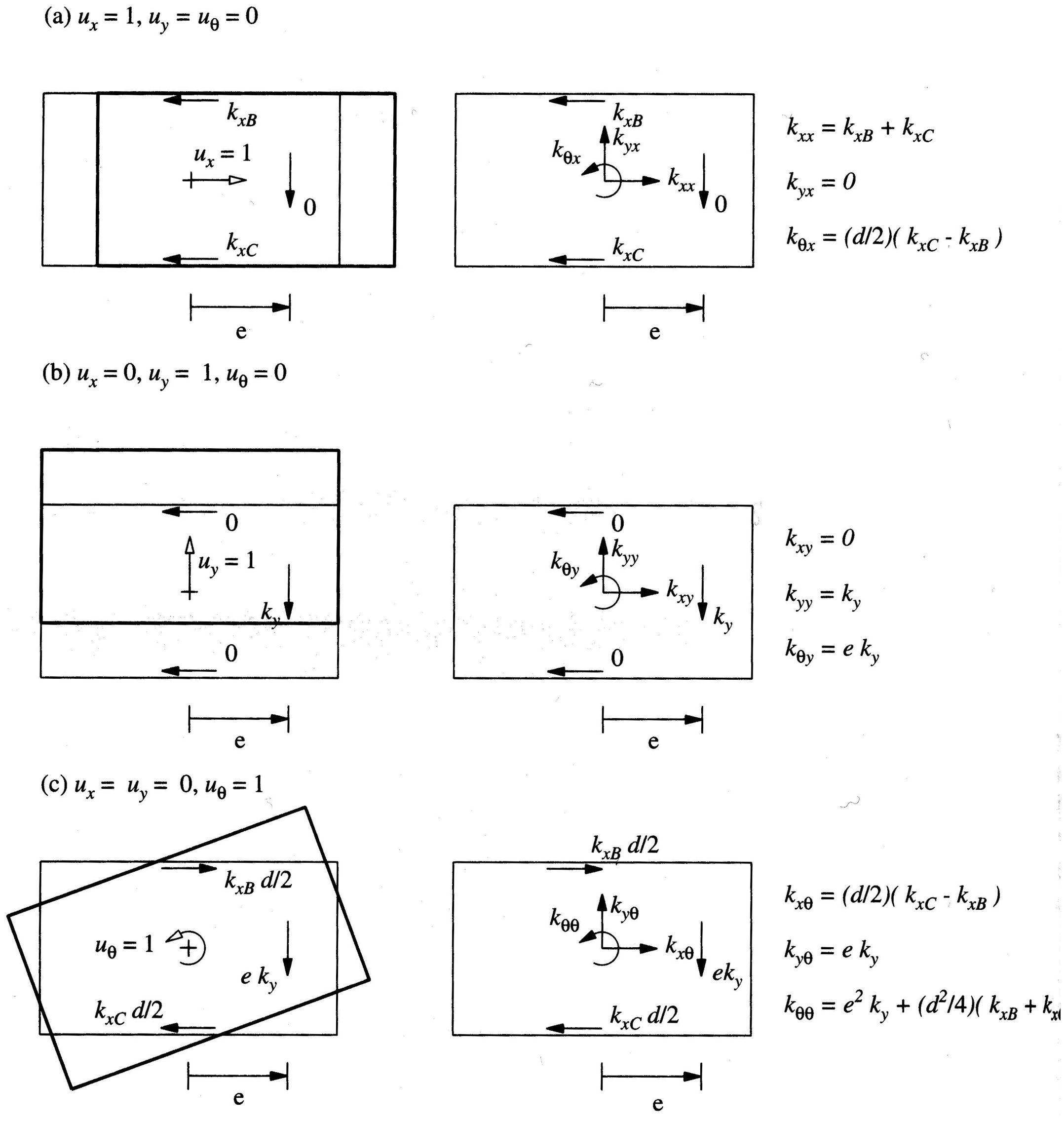
(a) u_x = 1, u_y = u_θ = 0
k_xB
u_x = 1
0
k_xC
e
k_xB
k_yx
k_θx
k_xx
0
k_xC
e
k_xx = k_xB + k_xC
k_yx = 0
k_θx = (d/2)(k_xC - k_xB)
(b) u_x = 0, u_y = 1, u_θ = 0
0
u_y = 1
k_y
0
e
0
k_yy
k_θy
k_xy
k_y
0
e
k_xy = 0
k_yy = k_y
k_θy = e k_y
(c) u_x = u_y = 0, u_θ = 1
k_xB d/2
u_θ = 1
e k_y
k_xC d/2
e
k_xB d/2
k_yθ
k_θθ
k_xθ
ek_y
k_xC d/2
e
k_xθ = (d/2)(k_xC - k_xB)
k_yθ = e k_y
k_θθ = e² k_y + (d²/4)(k_xB + k_x

Figure 3.8: Imposed unit displacements to construct k [3]

m is the diaphragm mass distributed uniformly over the plan, the moment of inertia about the z-axis going through O is $I_O = m(b^2+d^2)/12$ and $\ddot{u}_x^t$,$\ddot{u}_y^t$ and $\ddot{u}_\theta^t$ are the components of the total acceleration of the CM. The relationship between the inertia forces and accelerations are related through the mass matrix as shown here

$$\begin{bmatrix} f_{Ix} \\ f_{Iy} \\ f_{I\theta} \end{bmatrix} = \begin{bmatrix} m & 0 & 0 \\ 0 & m & 0 \\ 0 & 0 & I_O \end{bmatrix} \begin{bmatrix} \ddot{u}_x^t \\ \ddot{u}_y^t \\ \ddot{u}_\theta^t \end{bmatrix} \quad \text{or} \quad \mathbf{f}_I = \mathbf{m}\ddot{\mathbf{u}}^t \tag{3.40}$$

Using the information presented above, the equation of motion can be assembled. The total acceleration $\ddot{u}^t$ can be expanded to $\ddot{u}^t = \ddot{u} + \ddot{u}_g$. This gives

$$\begin{bmatrix} m & 0 & 0 \\ 0 & m & 0 \\ 0 & 0 & I_O \end{bmatrix} \begin{bmatrix} \ddot{u}_x \\ \ddot{u}_y \\ \ddot{u}_\theta \end{bmatrix} + \begin{bmatrix} k_{xB}+k_{xC} & 0 & (d/2)(k_{xC}-k_{xB}) \\ 0 & k_y & ek_y \\ (d/2)(k_{xC}-k_{xB}) & ek_y & e^2k_y + (d^2/4)(k_{xB}+k_{xC}) \end{bmatrix} \begin{bmatrix} u_x \\ u_y \\ u_\theta \end{bmatrix}$$

$$= -\begin{bmatrix} m\ddot{u}_{gx}(t) \\ m\ddot{u}_{gy}(t) \\ I_O\ddot{u}_{g\theta}(t) \end{bmatrix} \tag{3.41}$$

Here it is easy to spot that the governing DOFs are coupled through the stiffness matrix. This makes the system respond in DOFs different from the one where the load is applied. For example an acceleration in the y-direction will also cause lateral displacement both in the x and y direction, and also a torsional response.

3.2.2 Multi-story One Way Asymmetric System

In this section a system, from Chopra [3], with N floors that are symmetric about the x-axis but not the y-axis and where the jth floor has three DOFs, namely u_{jx}, u_{jy} and $u_{j\theta}$, will be presented. Since the x-motion is uncoupled to the two other DOFs, it can be solved alone. This gives a coupled lateral motion described by $2N$ DOFs. The displacement vector $\mathbf{u}$ has the size $2N\times$ 1.

$$\mathbf{u} = \begin{bmatrix} \mathbf{u}_y \\ \mathbf{u}_\theta \end{bmatrix} \tag{3.42}$$

where

$$\mathbf{u}_y = \begin{bmatrix} u_{1y} \\ u_{2y} \\ \vdots \\ u_{Ny} \end{bmatrix} \quad \mathbf{u}_\theta = \begin{bmatrix} u_{1\theta} \\ u_{2\theta} \\ \vdots \\ u_{N\theta} \end{bmatrix} \tag{3.43}$$

To obtain the stiffness matrix of such a system the direct stiffness method can be used, going through four steps listed in Chopra [3].

Step 1 Determine the lateral stiffness matrix for each frame. For the ith frame it is determined as follows. Define the DOF for the ith frame: lateral displacement at floor levels, $\mathbf{u}_i$, and vertical displacements and rotation for each node. Then the complete stiffness matrix for frame i with reference to the frames DOF. Then using statical condensation to condense all the rotational and vertical DOF to obtain the $N \times N$ lateral stiffness matrix of the ith frame, denoted $\mathbf{k}_{xi}$ or $\mathbf{k}_{yi}$ for a frame in the x or y-direction respectively.

Step 2 Determine the displacement transformation matrix relating the lateral DOF $\mathbf{u}_i$ defined in step 1 for the ith frame to get the global DOF $\mathbf{u}$ for the building. This $N \times 2N$matrix is denoted by $\mathbf{a}_{xi}$ or $\mathbf{a}_{yi}$. Thus:

$$\mathbf{u}_i = \mathbf{a}_{xi}\mathbf{u} \quad \text{or} \quad \mathbf{u}_i = \mathbf{a}_{yi}\mathbf{u} \tag{3.44}$$

These transformation matrices are

$$\mathbf{a}_{xi} = \begin{bmatrix} \mathbf{0} & -y_i\mathbf{I} \end{bmatrix} \quad \text{or} \quad \mathbf{a}_{yi} \begin{bmatrix} \mathbf{I} & x_i\mathbf{I} \end{bmatrix} \tag{3.45}$$

Where x_i and y_i define the location of the ith frame oriented in the y and x directions respectively. $\mathbf{I}$ is an identity matrix of order N and $\mathbf{0}$ is a square matrix of N elements, all equal to zero.

Step 3 Transform the lateral stiffness matrix for the ith frame to the building DOF $\mathbf{u}$ to obtain

$$\mathbf{k}_i = \mathbf{a}_{xi}^T\mathbf{k}_{xi}\mathbf{a}_{xi} \quad \text{or} \quad \mathbf{k}_i = \mathbf{a}_{yi}^T\mathbf{k}_{yi}\mathbf{a}_{yi} \tag{3.46}$$

Step 4 Add the stiffness matrices for all frames to obtain the stiffness matrix for the building

$$\mathbf{k} = \sum_i \mathbf{k}_i \tag{3.47}$$

Substituting equation (3.45) into equation (3.46) and the latter into equation (3.47) leads to

$$\mathbf{k} = \begin{bmatrix} \mathbf{k}_{yy} & \mathbf{k}_{y\theta} \\ \mathbf{k}_{\theta y} & \mathbf{k}_{\theta\theta} \end{bmatrix} \tag{3.48}$$

where

$$\mathbf{k}_{yy} = \sum_i \mathbf{k}_{yi} \quad \mathbf{k}_{y\theta} = \mathbf{k}_{\theta y}^T = \sum_i x_i\mathbf{k}_{yi} \quad \mathbf{k}_{\theta\theta} = \sum_i (x_i^2\mathbf{k}_{yi} + y^2\mathbf{k}_{xi}) \tag{3.49}$$

The equation of undamped motion of the structure subjected to ground acceleration $\ddot{u}_{gy}(t)$ can be developed as follows

$$\begin{bmatrix} \mathbf{m} & 0 \\ 0 & \mathbf{I}_O \end{bmatrix} \begin{bmatrix} \ddot{\mathbf{u}}_y \\ \ddot{\mathbf{u}}_\theta \end{bmatrix} + \begin{bmatrix} \mathbf{k}_{yy} & \mathbf{k}_{y\theta} \\ \mathbf{k}_{\theta y} & \mathbf{k}_{\theta\theta} \end{bmatrix} \begin{bmatrix} \mathbf{u}_y \\ \mathbf{u}_\theta \end{bmatrix} = - \begin{bmatrix} \mathbf{m} & 0 \\ 0 & \mathbf{I}_O \end{bmatrix} \begin{bmatrix} \mathbf{1} \\ \mathbf{0} \end{bmatrix} \ddot{u}_{gy}(t) \tag{3.50}$$

In equation (3.50) $\mathbf{m}$ is a diagonal matrix of order N, with $m_{jj} = m_j$ the mass lumped at the jth floor diaphragm, $\mathbf{I}_O$ is a diagonal matrix of the Nth order with $I_{jj} = I_{Oj}$, the moment of inertia of the jth floor diaphragm about the vertical axis through the center of mass. $\mathbf{1}$ and $\mathbf{0}$ are vectors of dimension N with elements equal to 1 and 0, respectively.

If all diaphragms are of the same size and weight, the equation simplifies to this

$$\begin{bmatrix} \mathbf{m} & 0 \\ 0 & \mathbf{I}_O \end{bmatrix} \begin{bmatrix} \ddot{\mathbf{u}}_y \\ \ddot{\mathbf{u}}_\theta \end{bmatrix} + \begin{bmatrix} \mathbf{k}_{yy} & \mathbf{k}_{y\theta} \\ \mathbf{k}_{\theta y} & \mathbf{k}_{\theta\theta} \end{bmatrix} \begin{bmatrix} \mathbf{u}_y \\ \mathbf{u}_\theta \end{bmatrix} = - \begin{bmatrix} \mathbf{m} & 0 \\ 0 & r^2\mathbf{m} \end{bmatrix} \begin{bmatrix} \mathbf{1} \\ \mathbf{0} \end{bmatrix} \ddot{u}_{gy}(t) \tag{3.51}$$

To perform a modal analysis of the system, a modal expansion of the effective earthquake forces have to be done, similar to the symmetric plan structure. The effective forces $\mathbf{p}_{eff}(t)$ are defined by the right side of equation (3.51)

$$\mathbf{p}_{eff}(t) = - \begin{bmatrix} \mathbf{m1} \\ \mathbf{0} \end{bmatrix} \ddot{u}_{gy}(t) \equiv -\mathbf{s}\ddot{u}_{gy}(t) \tag{3.52}$$

The summation of of modal inertia force distributions $\mathbf{s_n}$ are the expansion of the spatial distribution $\mathbf{s}$

$$\begin{bmatrix} \mathbf{m1} \\ \mathbf{0} \end{bmatrix} = \sum_{n=1}^{2N} \mathbf{s}_n = \sum_{n=1}^{2N} \Gamma_n \begin{bmatrix} \mathbf{m}\phi_{yn} \\ r^2\mathbf{m}\phi_{\theta n} \end{bmatrix} \tag{3.53}$$

Here ϕ_{yn} and $\phi_{\theta n}$ contains the translations and rotations, respectively. of the N floors about a vertical axis in the nth mode.

The modal participation factor is then found

$$\Gamma_n = \frac{L_n^h}{M_n} \tag{3.54}$$

where

$$L_n^h = [\phi_{yn}^T \quad \phi_{\theta n}^T] \begin{bmatrix} \mathbf{m1} \\ \mathbf{0} \end{bmatrix} = \phi_{yn}^T \mathbf{m1} = \sum_{j=1}^{N} m_j \phi_{jyn} \tag{3.55}$$

and

$$M_n = [\phi_{yn}^T \quad \phi_{\theta n}^T] \begin{bmatrix} \mathbf{m} & 0 \\ 0 & r^2\mathbf{m} \end{bmatrix} \begin{bmatrix} \phi_{yn} \\ \phi_{\theta n} \end{bmatrix} \tag{3.56}$$

or

$$M_n = \phi_{yn}^T \mathbf{m} \phi_{yn} + r^2 \phi_{\theta n}^T \mathbf{m} \phi_{\theta n} = \sum_{j=1}^{N} m_j \phi_{jyn}^2 + r^2 \sum_{j=1}^{N} m_j \phi_{j\theta n}^2 \tag{3.57}$$

j denotes the floor number and m_j the floor mass.

The lateral force, s_{jyn}, and torque, $s_{j\theta n}$, at the jth floor level is expressed as follows

$$s_{jyn} = \Gamma_n m_j \phi_{jyn} \quad s_{j\theta n} = \Gamma_n r^2 m_j \phi_{j\theta n} \tag{3.58}$$

The lateral and torsional displacements are

$$\mathbf{u}_{yn}(t) = \Gamma_n \phi_{yn} D_n(t) \quad \mathbf{u}_{\theta n}(t) = \Gamma_n \phi_{\theta n} D_n(t) \tag{3.59}$$

The equivalent static forces $\mathbf{f}_n$ as a result of the displacements $\mathbf{u}_n(t)$ include lateral and torsional forces.

$$\begin{bmatrix} \mathbf{f}_{yn}(t) \\ \mathbf{f}_{\theta n}(t) \end{bmatrix} = \begin{bmatrix} \mathbf{s}_{yn} \\ \mathbf{s}_{\theta n} \end{bmatrix} A_n(t) \tag{3.60}$$

The response to the nth mode is given as mentioned in equation (3.21) and repeated here

$$r_n(t) = r_n^{st} A_n(t) \tag{3.61}$$

Selected modal static responses are presented in table 3.3

Table 3.3: Modal Static Responses [3]

Response, r	Modal Static Response, r_n^{st}
V_i	$V_{in}^{st} = \sum_{j=i}^{N} s_{jyn}$
M_i	$M_{in}^{st} = \sum_{j=i}^{N} (h_j - h_i) s_{jyn}$
T_i	$T_{in}^{st} = \sum_{j=i}^{N} s_{j\theta n}$
V_b	$V_{bn}^{st} = \sum_{j=1}^{N} s_{jyn} = \Gamma_n L_n^h = M_n^*$
M_b	$M_{bn}^{st} = \sum_{j=1}^{N} h_j s_{jyn} = \Gamma_n L_n^\theta = h_n^* M_n^*$
T_b	$T_{bn}^{st} = \sum_{j=1}^{N} s_{j\theta n} I_{On}^*$
u_{jy}	$u_{jyn}^{st} = (\Gamma_n / \omega_n^2) \phi_{jyn}$
$u_j\theta$	$u_{j\theta n}^{st} = (\Gamma_n / \omega_n^2) \phi_{j\theta n}$

To get the forces of the elements in the structure the lateral displacements of each frame in the building is connected to the floor displacement through equation (3.44). Substituting equation (3.45) for $\mathbf{a}_{xi}$ and $\mathbf{a}_{yi}$, $\mathbf{u}_n^T = [\mathbf{u}_{yn}^T \quad \mathbf{u}_{\theta n}^T]$ and equation (3.59) for $\mathbf{u}_{yn}$ and $\mathbf{u}_{\theta n}$ provides

$$\mathbf{u}_{in}(t) = \Gamma_n(-y_i\phi_{\theta n})D_n(t) \qquad \mathbf{u}_{in}(t) = \Gamma_n(\phi_{yn} + x_i\phi_{\theta n})D_n(t) \tag{3.62}$$

The expressions in equation (3.62) are for frames in the x- and y-direction, respectively. The total response can then be found by summing up the modal contributions.

$$r(t) = \sum_{n=1}^{2N} r_n(t) = \sum_{n=1}^{2N} r_n^{st} A_n(t) \tag{3.63}$$

A summary of how to adapt this to response spectrum analysis was made by Chopra [3] and quoted here

1. Define the structural properties
   (a) Determine the mass and stiffness matrices from equation (3.51) and (3.49)
   (b) Estimate the modal damping ratios ζ_n
2. Determine the natural frequencies ω_n and natural modes of vibration, ϕ_n
3. Compute the peak response in the nth mode by the following steps, repeated for all modes, $n = 1, 2, ..., 2N$
   (a) Corresponding to the natural period T_n and damping ratio ζ_n, read D_n and A_n from the earthquake response spectrum, or the design spectrum.
   (b) Compute the lateral displacements and rotations of the floors from equation (3.59)
   (c) Compute the equivalent static forces: Lateral forces $\mathbf{f}_{yn}$ and torques $\mathbf{f}_{\theta n}$ from equation (3.60)
   (d) Compute the story forces by three dimensional static analysis of the structure subjected to external forces $\mathbf{f}_{yn}$ and $\mathbf{f}_{\theta n}$
4. Determine an estimate for the peak value r of any response quantity by combining the peak modal values r_n. The CQC-rule is explained in section 3.1.2

3.2.3 Response Spectrum Analysis of an Asymmetric Plan Structure

In this section a model with asymmetric plans has been modelled in SAP2000. The influence of the choice of modal combination rule on the results from a response spectrum analysis will be controlled.

The system investigated is shown in figure 3.9

The left frame consists of HE200A beams and columns, while the two to the right consists of HE120A. The floor is C35 concrete. The total weight of the structure is 352 422 kg. It is subjected to the El Centro ground motion shown in figure 2.3 and the response spectrum

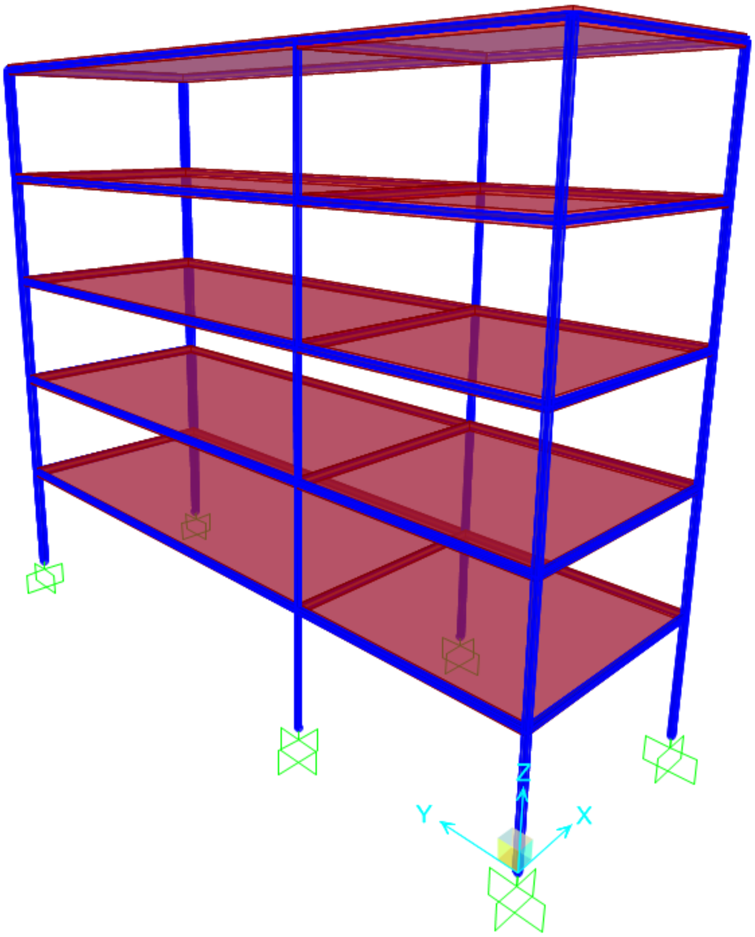

Figure 3.9: SAP2000 System

shown in figure 3.5. The response spectrum results have been found using both SRSS and CQC to investigate the difference between the two. The load has been applied in the x-direction, which is parallel to the short side of the system.

The modal period of the system is listed in table 3.4

In table 3.5 base shear and displacement of joint 35, the top left joint in figure 3.9, has been listed.

Table 3.4: Modal Periods

Mode	Period
1	3.450248 sec
2	2.97132 sec
3	1.509088 sec
4	1.16982 sec
5	1.01603 sec
6	0.728498 sec
7	0.640462 sec
8	0.5561 sec
9	0.514713 sec
10	0.49744 sec
11	0.480185 sec
12	0.435423 sec

Table 3.5: Comparison of CQC and SRSS

Modal Combination Rule	Base Shear	Joint Disp X	Joint Disp Y
SRSS (5% Damping)	349.958 kN	0.1299 m	0.3667 m
CQC (5% Damping)	364.678 kN	0.1313 m	0.3671 m
SRSS (20% Damping)	229.416 kN	0.0851 m	0.2404 m
CQC (20% Damping)	290.581 kN	0.0866 m	0.2411 m

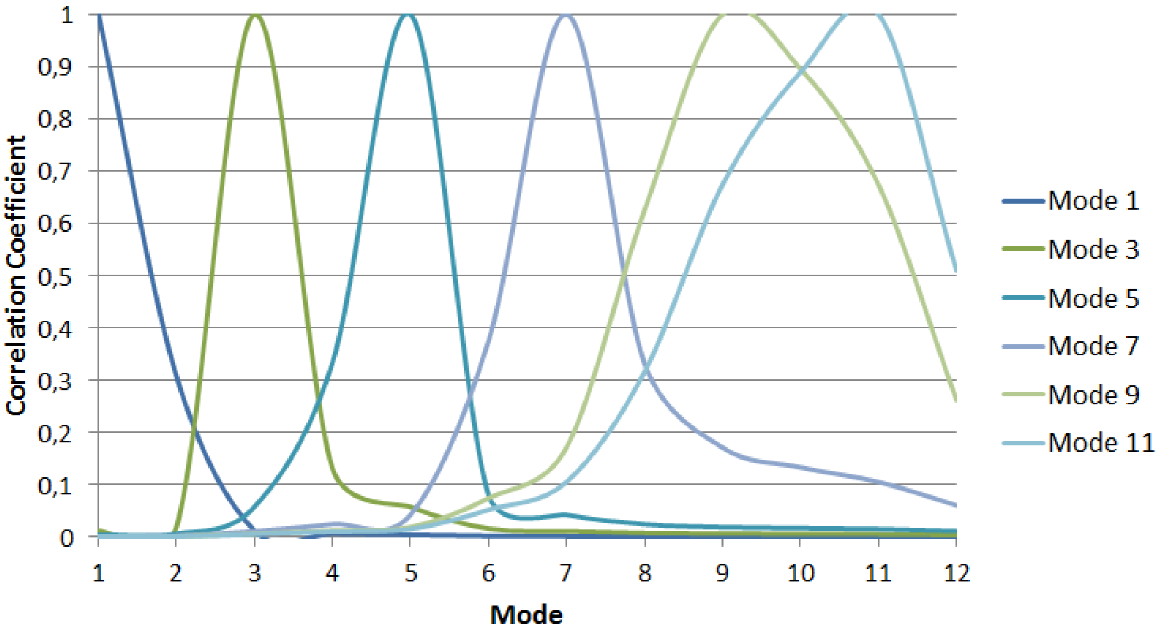

Figure 3.10: Correlation coefficient for 5% damping

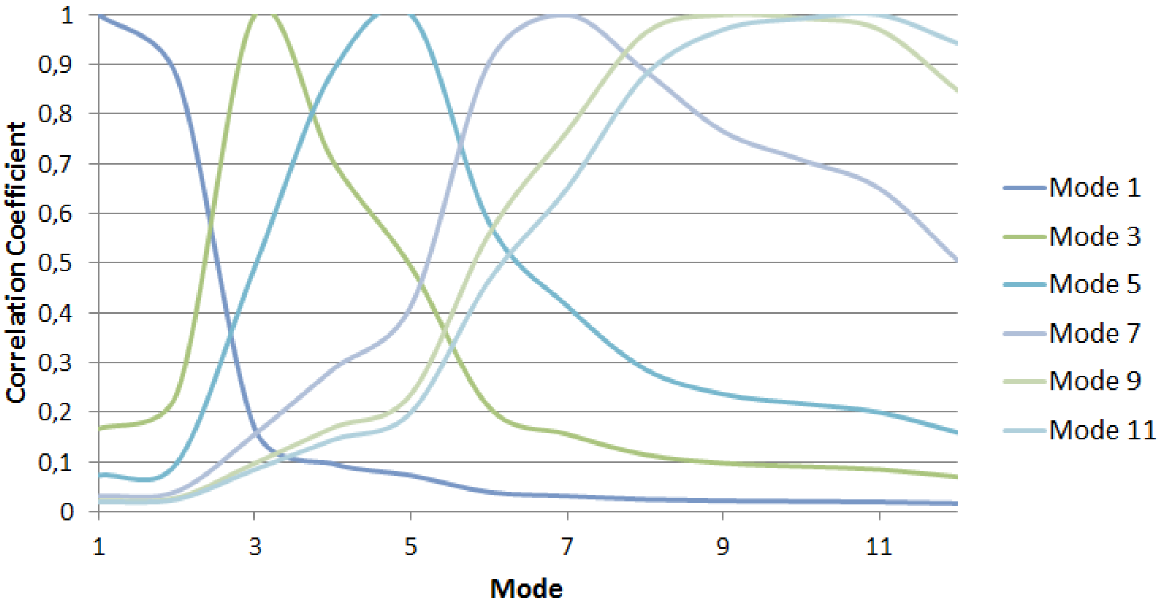

Figure 3.11: Correlation coefficient for 20 % damping

The results show that there is a slight difference in the results. They are especially pronounced in the base shear. As shown in figure 3.2 the damping influences the correlation coefficient. This is illustrated with the results found when the analysis is run with 20% modal damping. In figure 3.10 and 3.11 the correlation coefficient is shown graphically for the 5% and 20% modal damping case, respectively. The wider curves in figure 3.11 illustrates how the different modes influences over a wider area of the spectrum, compared to the 5% case. It also illustrates that the closely spaced last modes affect each other more, than the more spread early ones, as listed in table 3.4. Equation (3.25) was used to calculate the coefficients.

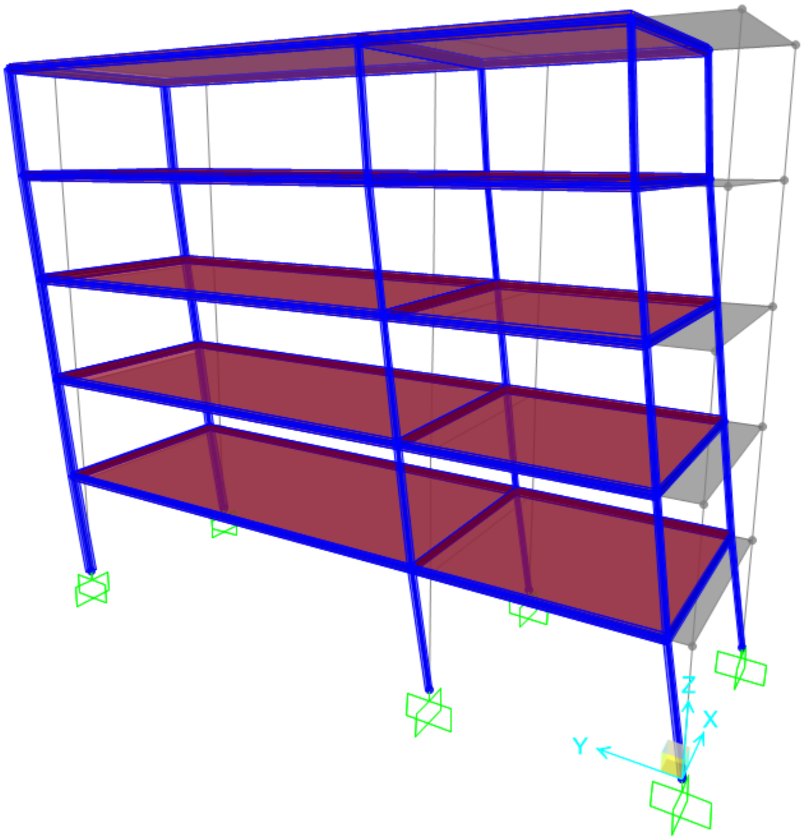

Figure 3.12: Envelope of deformation for Linear Modal History Analysis in Y-direction

The symmetry in the y-direction causes, as the theory claims, no rotation or translation in the orthogonal direction, an envelope of the linear modal history analysis in the y-direction is shown in figure 3.12

Chapter 4

Inelastic Analysis

This chapter will present the procedure to perform inelastic modal pushover analysis both for symmetric and asymmetric plan systems. Factors that needs to be included in an analysis will also be discussed and a modal pushover analysis will be performed on a 2D frame. The theory is adapted from Chopra [3], Gupta and Krawinkler [8], [10], Chopra and Goul [9], [12].

For an inelastic system the relationship between lateral forces **s** and displacements u are not single-valued, but depend on the history of the displacement.

$$\mathbf{f}_s = \mathbf{f}_s(\mathbf{u}, \text{sign}\dot{\mathbf{u}}) \tag{4.1}$$

The loading and unloading curves differs from the initial loading branch, and experiments on structural elements have provided force-deformation relations appropriate for different elements and materials. With the generalization in equation (4.1) the equation of motion becomes

$$\mathbf{m}\ddot{\mathbf{u}} + \mathbf{c}\dot{\mathbf{u}} + \mathbf{f}_s(\mathbf{u}, \dot{\mathbf{u}}) = -\mathbf{m}\iota\ddot{u}_g(t) \tag{4.2}$$

This matrix equation represents N non-linear differential equations for N floor displacements $u_j(t), j = 1, 2, ..., N$. With a given mass- and damping matrix combined with the inelastic force-deformation relationship, $\mathbf{f}_s(\mathbf{u}, \dot{\mathbf{u}})$ and ground acceleration $\ddot{u}_g$, a numerical solution of equation (4.2) is needed to acquire the displacement response of the structure.

Solving this equation is very computationally demanding. The stiffness matrix has to be reformulated at each time step, according to the deformation and state of each structural element. For large structures this process has to be repeated for a very large number of elements. In addition non-linear geometry has to be considered, since structures subjected to intense ground motions can undergo large displacement, causing P-Δ-effects.

To obtain usable result for inelastic response of a structure, a number of factors should be included. In addition to the previously mentioned P-Δ-effects, there are idealization assumptions and ground motion characteristics.

P-Δ-effects is the name for second-order effects of downwards gravity caused by lateral deformation of the structure. As shown by Gupta and Krawinkler [8] in figure 4.1 the inclusion of this effect greatly changes the pushover curve. The initial stiffness is almost equal, showing that it is negligible in elastic analysis, but when it moves into the inelastic range the differences starts to show. While the post-yield stiffness remains positive without

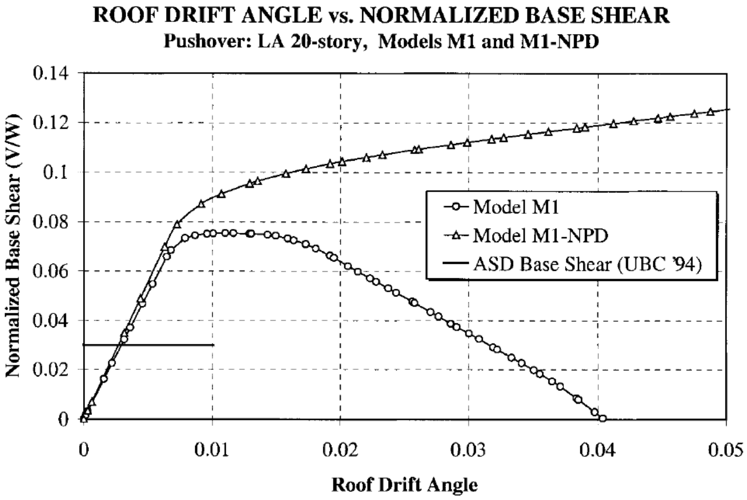

Figure 4.1: Global Pushover Curve of 20 Story Building LA, with and without P-delta [8]

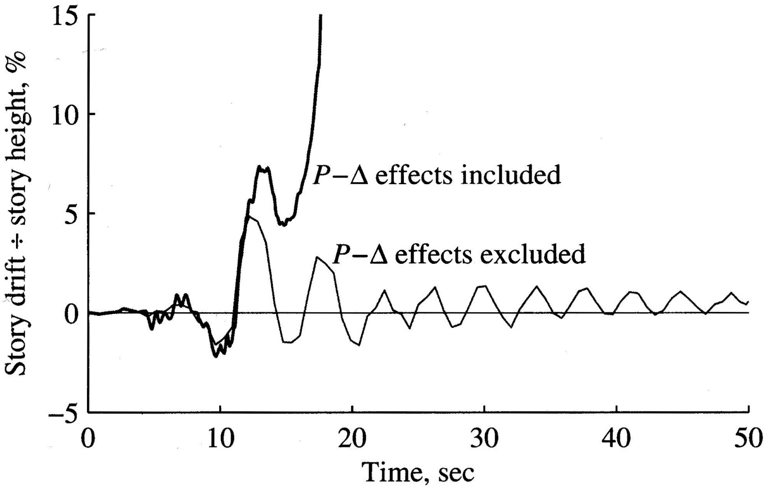

Figure 4.2: Effects of P-delta effects [3]

the P-Δ-effects, the opposite happens when they are included, and after a short constant strength plateau, the stiffness reduces quickly, getting to zero when the roof displacement is 4% of the building height when used on a SAC-LA 20-story building. This can also be shown with a response to a time history load, in figure 4.2

The way in which a structure is modelled and the idealizations used in the process can greatly influence the inelastic response of a structure. To demonstrate this effect the work of Gupta and Krawinkler will be used again [8]. In their work on the SAC-Los Angeles 20-story building they demonstrated the difference in response from three different planar idealization of the frames considered. The first model, named M1 is a basic centreline model where the panel zones strength, size and stiffness are ignored. The second model (M2) explicitly includes the strength and stiffness properties of the panel zones, and the third model (M2A) is a further enhanced version of model two, including interior gravity columns, shear connections and floor slabs.

These modelling differences will cause a large difference in the response to an earthquake load. Figure 4.3 shows the drift demands for each story with model M2 and M2A. Model

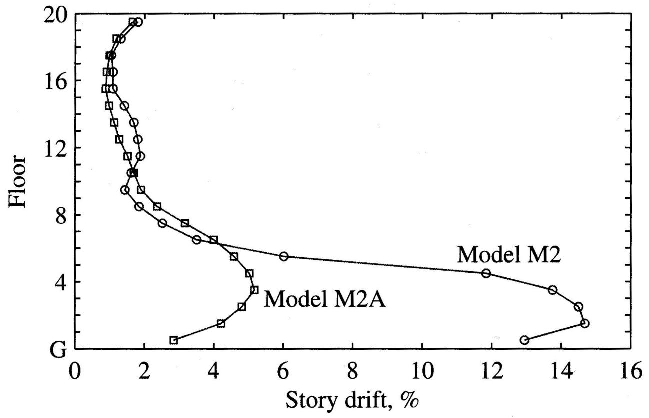

Figure 4.3: Influence on story drifts by modelling [3]

M1 went to failure, so that one is not included in the figure.

There is also variation in the different ground motions. This causes a statistical variation. Figure 4.4 shows the statistical drift demands for three ensembles of ground motion with a return period of 2475 years (2/50), 475 years (10/50) and 72 years (50/50). It is observed that with increasing intensity of the ground motion, a larger dispersion of the demand is obtained.

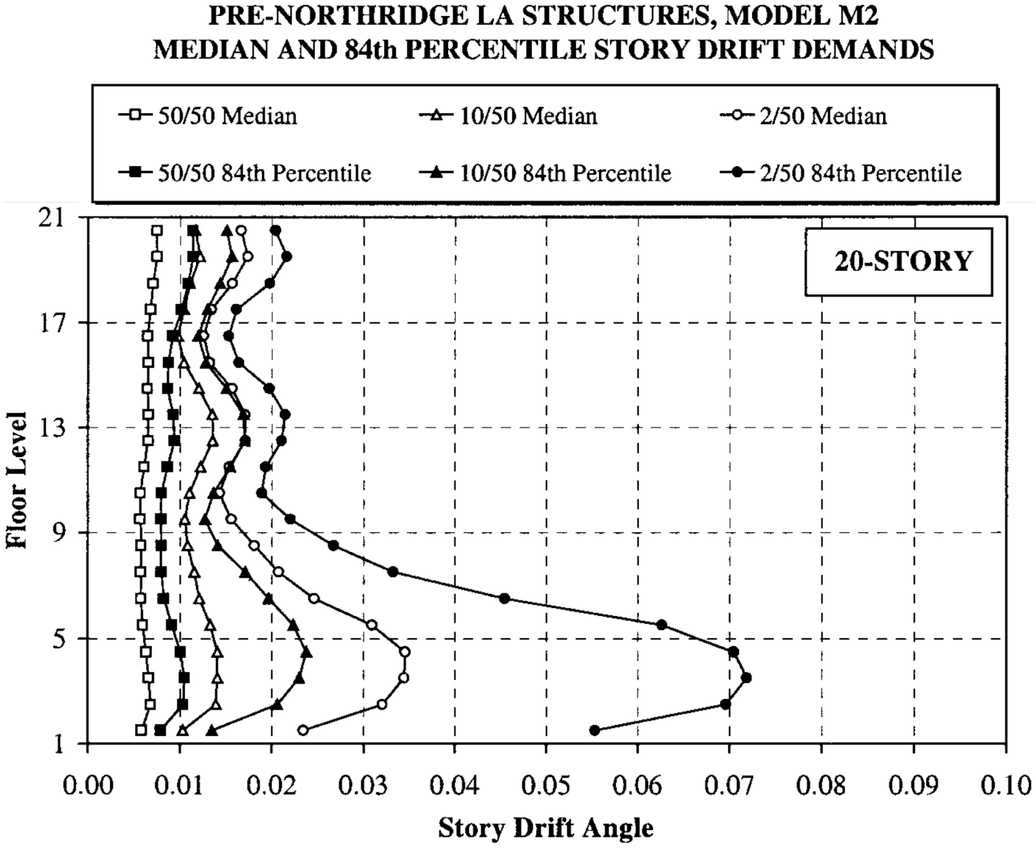

Figure 4.4: Statistical values of story drift demands for LA-Structure M2 Model [10]

4.1 Response History Analysis

This section presents the equation of motion for a non-linear MDOF system by theory adapted from Chopra [3] and Chopra and Goel [9]. When doing the response history analysis equation (4.2) is expanded using the natural vibration modes of the corresponding linear system getting

$$\mathbf{u}(t) = \sum_{n=1}^{N} \boldsymbol{\phi}_n q_n(t) \tag{4.3}$$

Equation (4.3) is then substituted into equation (4.2) and pre-multiplied with $\boldsymbol{\phi}_n^T$. Using mass and classical damping orthogonality the following equation is obtained

$$\ddot{q}_n + 2\zeta_n \omega_n \dot{q}_n + \frac{F_{sn}}{M_n} = -\Gamma_n \ddot{u}_g(t), \quad n = 1, 2, ..., N \tag{4.4}$$

Here the only thing different from equation (3.16) is

$$F_{sn} = F_{sn}(\mathbf{q}, \text{sign}\dot{\mathbf{q}}) = \boldsymbol{\phi}_n^T \mathbf{f}_s(\mathbf{u}, \text{sign}\dot{\mathbf{u}}) \tag{4.5}$$

The resisting force now depends on all modal coordinates $q_n(t)$, implying the coupling of modal coordinates because of yielding of the structure. Unlike equation (3.16) equation (4.4) consists of N coupled equations.

4.2 Uncoupled Modal Response History Analysis

When neglecting the coupling of modes the uncoupled modal response history analysis can be obtained. This simplification is the basis from where modal pushover analysis has been derived. This theory is adapted from Chopra and Goel [9]

The spatial distribution of the effective earthquake forces, $\mathbf{s}$, is expanded into modal contribution $\mathbf{s}_n$ according to equation (3.12), repeated here for convenience

$$\mathbf{s} = \sum_{n=1}^{N} \mathbf{s}_n = \sum_{n=1}^{N} \Gamma_n \mathbf{m} \phi_n$$

$\boldsymbol{\phi}_n$ is still the modes of the corresponding linear system and the governing equation of motion for this inelastic system is given by this

$$\mathbf{m}\ddot{\mathbf{u}} + \mathbf{c}\dot{\mathbf{u}} + \mathbf{f}_s(\mathbf{u}, \text{sign}\dot{\mathbf{u}}) = -\mathbf{s}_n \ddot{u}_g(t) \tag{4.6}$$

The solution of equation (4.6) can not exactly be solved by the help of equation (3.19) because the inelastic properties will cause other modes than the nth mode to influence the response.

This is where one of the simplifications in this method comes in, and the coupling is assumed to be negligible. The effect of this action has been illustrated numerically by Chopra and Goel [9] on a 9 story SAC-building. They solved the problem numerically with non-linear

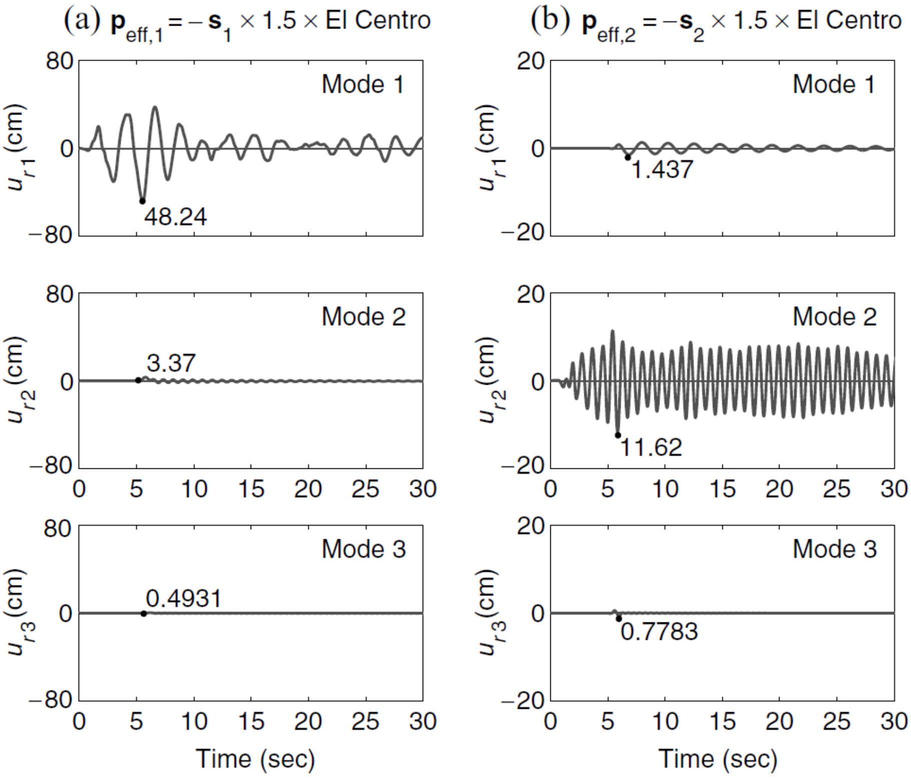

Figure 4.5: Modal Decomposition of the roof displacement [9]

RHA and decomposed the resulting roof displacement history into its "modal" components. The model was subjected to 1.5 times El Centro ground motion and all but two beams yielded.

The second and third mode started responding to $\mathbf{p}_{\mathrm{eff},1}(t)$ the moment the structure yielded, but their contribution to roof displacement were a mere 7% for mode two and 1% for mode three. The response to $\mathbf{p}_{\mathrm{eff},2}(t)$ yielded a contribution from mode one at 12% and 7% for mode three. Figure 4.5 illustrates this.

This approximation changes F_{sn} from equation (4.5) so that it only depends on one modal coordinate, q_n.

$$F_{sn} = F_{sn}(q_n, \mathrm{sign}\dot{q}_n) = \boldsymbol{\phi}_n^T \mathbf{f}_s(q_n, \mathrm{sign}\dot{q}_n) \tag{4.7}$$

By using this, the solution of equation (4.4) can be expressed with equation (3.18) yielding

$$\ddot{D}_n + 2\zeta_n\omega_n\dot{D}_n + \frac{F_{sn}}{L_n} = -\ddot{u}_g(t) \tag{4.8}$$

and

$$F_{sn} = F_{sn}(D_n, \mathrm{sign}\dot{D}_n) = \boldsymbol{\phi}_n^T \mathbf{f}_s(D_n, \mathrm{sign}\dot{D}_n) \tag{4.9}$$

Equation (4.8) can be interpreted as the governing equation of the nth "mode" inelastic SDOF-system, this system has the damping ratio ζ_n and natural frequency ω_n of the corresponding linear MDOF-systems nth mode, and the $F_{sn}/L_n - D_n$ relation between resisting forces F_{sn}/L_n and modal coordinate D_n defined by equation (4.9). The F_{sn}/L_n-curve is found using the procedure showed in section 4.3

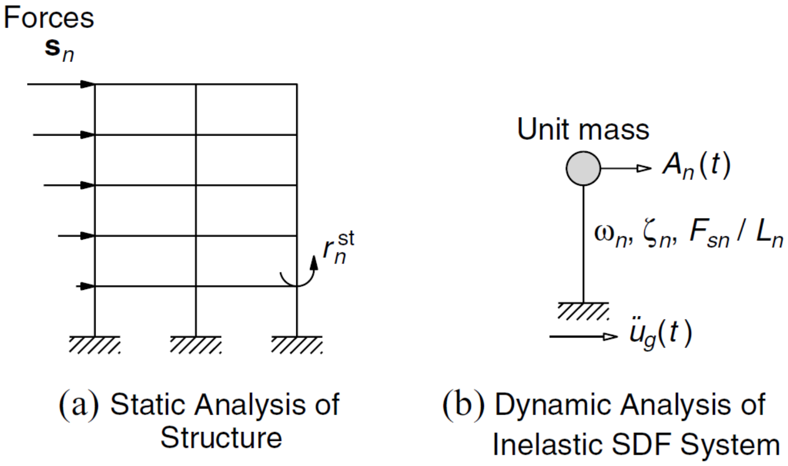

(a) Static Analysis of Structure

(b) Dynamic Analysis of Inelastic SDF System

Figure 4.6: Conceptual explanation of uncoupled modal RHA of inelastic MDOF systems [9]

The use of equation (4.8) is preferable compared to equation (4.4) because it is on the same form as a standard equation for a SDOF-system, and the peak value can be estimated from the inelastic response, or design, spectrum.

Solution of equation (4.8) written like this provides $D_n(t)$, which when substituted into equation (3.19) gives the floor displacements associated with the nth "mode" inelastic SDOF-system. Other deformation quantities $r_n(t)$ is given by the following equations

$$r_n(t) = r_n^{st} A_n(t) \tag{4.10}$$

$$A_n(t) = \omega_n^2 D_n(t) \tag{4.11}$$

$A_n(t)$ is now the pseudo-acceleration response of the nth "mode" inelastic SDOF-system. The two analysis leading to this have been described schematically by Chopra and Goel and is included as figure 4.6

Equation (4.10) and (4.11) now represent the response of inelastic MDOF system to $\mathbf{p}_{\text{eff,n}}(t)$, also known as the nth mode contribution to $\mathbf{p}_{\text{eff}}(t)$

The errors in UMRHA gets contribution from the three following assumptions and approximations.

- The coupling of modal coordinates is ignored.
- The superposition of responses to $\mathbf{p}_{\text{eff,n}}(t)$ is invalid for inelastic systems.
- The $F_{sn}/L_n - D_n$relationship is approximated via a bilinear curve.

4.3 Properties of the nth Mode Inelastic SDOF-system and Pushover Curve

To obtain the $F_{sn}/L_n - D_n$-curve a non-linear static analysis where the structure undergoes the displacement $\mathbf{u} = D_n\boldsymbol{\phi}_n$with increasing D_n has to be performed, but most software can not implement such a displacement controlled analysis. To work around this problem a force-controlled non-linear static analysis with invariant distribution of lateral forces can be used. The distribution fitting best to the purpose would be $\boldsymbol{\phi}_n$. When this is done in most software the result provided is the pushover curve, not the $F_{sn}/L_n - D_n$-curve. To convert this into the correct terms, the following equations have been derive

$$F_{sn} = \frac{V_{bn}}{\Gamma_n}, \quad D_n = \frac{u_{rn}}{\Gamma_n \phi_{rn}} \tag{4.12}$$

Equation (4.12) enables the conversion to the $F_{sn}/L_n - D_n$-curve from the pushover curve. The yield points in the pushover curve are

$$\frac{F_{sny}}{L_n} = \frac{V_{bny}}{M_n^*}, \quad D_{ny} = \frac{u_{rny}}{\Gamma_n \phi_{rn}} \tag{4.13}$$

$M_n^* = L_n \Gamma_n$ is the effective modal mass. The two are related through

$$\frac{F_{sny}}{L_n} = \omega_n^2 D_{ny} \tag{4.14}$$

This implies that the slope of the initial line in the $F_{sn}/L_n - D_n$-curve is ω_n^2. From the values defined the elastic period T_n of the nth "mode" inelastic system is calculated like this

$$T_n = 2\pi \left(\frac{L_n D_{ny}}{F_{sny}} \right)^{1/2} \tag{4.15}$$

4.4 Modal Pushover Analysis

While the Uncoupled Modal Response History Analysis is exact for elastic systems its weaknesses makes it less precise for inelastic system, and opening the use of Modal Pushover Analysis instead. The theory is adapted from Chopra [3] and Chopra and Goel [9]

The response r_n of an inelastic system subjected to effective earthquake forces $\mathbf{p}_{\text{eff},n}(t)$. Now a non-linear static analysis of the structure subjected to lateral forces distributed over the building height according to s_n^* with the structure pushed to the roof displacement u_{rno}. The value of roof displacement is given by equation (3.19) where D_n is determined by solving equation (4.8) and finding the maximum, or determining it from the inelastic design or response spectrum. Pushed to this roof displacement, the analysis provides estimated peak values of any response, for example floor displacements, story drifts, joint rotations and plastic hinge rotations. These are combined for the different modes using modal combination rules.

The difference between UMRHA and MPA is contained in their assumptions. UMRHA is based on the assumption that modal displacements are uncoupled. In the MPA analysis the displacements are calculated through a non-linear static analysis using the force distribution s_n^*. This causes the displacements not to be proportional to the mode shape, causing MPA to be more accurate for inelastic cases. MPA does contain another approximation not found in UMRHA which is the combination of responses through a modal combination rule of the modal responses, as done in the linear case.

The method can be summarized for a symmetric plan building on a step by step form as done by Chopra [3].

1. Compute the natural frequencies, ω_n, and modes, ϕ_n for linearly elastic vibration of the system
2. Develop the base shear-roof displacement pushover curve for mode n, $V_{bn} - u_{rn}$ by non-linear static analysis of the building using the force distribution s_n^*
3. Utilizing equation (4.13) to convert the $v_{bn} - u_{rn}$ pushover curve to the force deformation relation for the nth mode inelastic SDOF-system, $F_{sn}/L_n - D_n$
4. Idealize the F-D-relationship for the nth mode SDOF-system. For example as a bilinear curve.
5. Compute the peak deformation D_n of the nth mode SDOF-system. This is done by estimating the damping ratio and using equation (4.15) to find the inelastic vibration period. D_n is then determined using non-linear RHA or response/design spectrum.
6. Calculate the roof displacement u_{rn} associated with the nth mode inelastic SDOF system with equation (3.19)
7. From the pushover curve in step 2, extract values of desired responses r_{n+g} de to the combined effects of gravity and lateral loads at roof displacement equal to $u_{rn} + u_{rg}$
8. Repeat step 3 to 7 for as many modes as required for sufficient accuracy
9. Compute the dynamic response due to the nth mode: $r_n = r_{n+g} - r_g$, where r_g is the contribution to gravity loads alone
10. Determine the total dynamic response r_d by combining the peak modal responses using an appropriate modal contribution rule 3.1.2
11. Determine the total seismic demand by combining the initial static responses due to gravity loads and dynamic response.

4.4.1 Modal Pushover Analysis of a 2D Frame

This section will contain a modal pushover analysis of the frame analysed in section 3.1.4. The model is the same, and it will be subjected to a EC8 design spectrum with a_g equivalent to the peak acceleration of El Centro and 1.5xEl Centro. It will then be compared with direct integration time history analysis to control the accuracy.

The plastic hinges are assigned to both ends of all column and beams, according to FEMA356 Table 5-6 for columns and beams respectively. The hinges have the properties shown in figure 4.7.

The mode shapes of the system is shown in figure 4.8.

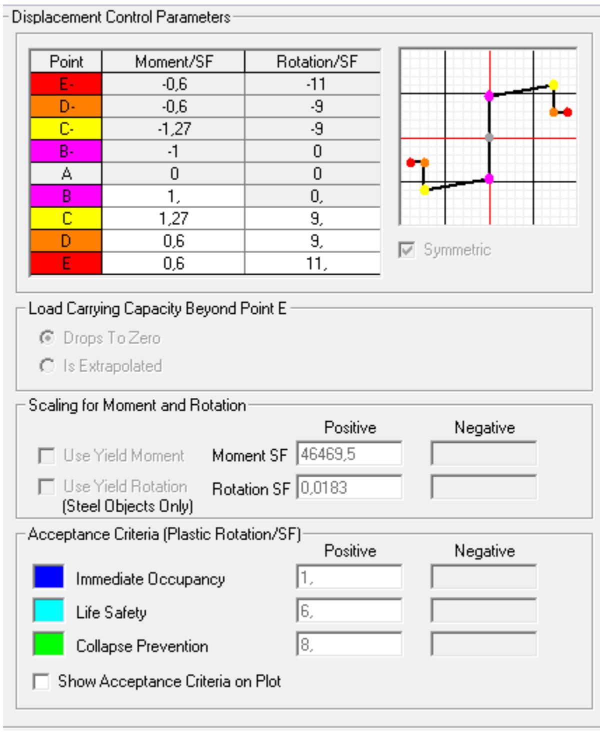

Displacement Control Parameters

Point	Moment/SF	Rotation/SF
E-	-0,6	-11
D-	-0,6	-9
C-	-1,27	-9
B-	-1	0
A	0	0
B	1,	0,
C	1,27	9,
D	0,6	9,
E	0,6	11,

☑ Symmetric

Load Carrying Capacity Beyond Point E

● Drops To Zero

○ Is Extrapolated

Scaling for Moment and Rotation

		Positive	Negative
☐ Use Yield Moment	Moment SF	46469,5	
☐ Use Yield Rotation (Steel Objects Only)	Rotation SF	0,0183	

Acceptance Criteria (Plastic Rotation/SF)

	Positive	Negative
🟦 Immediate Occupancy	1,	
🟦 Life Safety	6,	
🟩 Collapse Prevention	8,	

☐ Show Acceptance Criteria on Plot

Figure 4.7: Hinge Properties

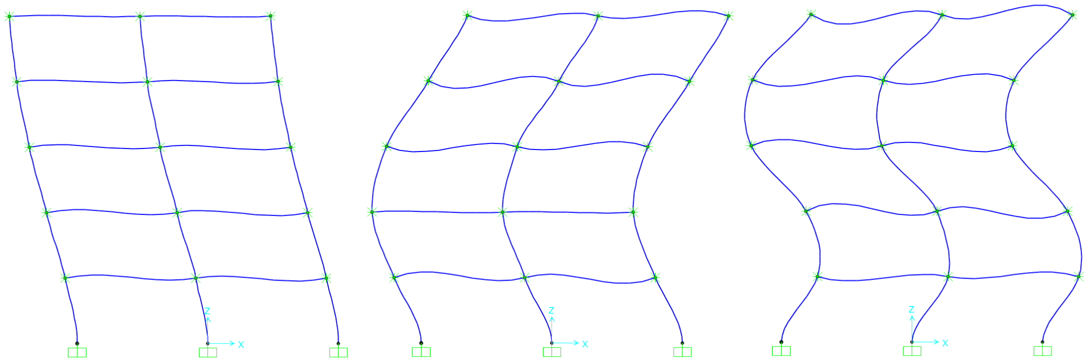

Figure 4.8: Mode shapes 1 through 3

Table 4.1: Modal Participation Factors

Mode	Modal Participation Factor, Γ_n
Mode 1	163.664
Mode 2	59.943
Mode 3	37.491
Mode 4	25.896
Mode 5	14.468

The structure is then subjected to 3 different loads, each distributed spatially equally to the mode shapes, giving the pushover curves and deformations displayed in figure 4.9 and 4.10 respectively. The colour codes for the plastic hinges are as follows:

- Pink: Yield
- Blue: Immediate occupancy
- Teal: Life Safety
- Green: Collapse prevention
- Yellow: Loss of strength
- Orange: Tearing
- Red: Fracture

The colours pink, yellow, orange and red can also be found in figure 4.7.

The roof displacement of mode 2 is very low, this is due to the shape of the mode. The modal coefficient on level 3 is almost equal to the modal coefficient on the roof, but in the opposite direction. When a load with that distribution is applied, they will counteract each-other, limiting the absolute roof displacement, while causing large story drifts. Only three modes have been included due to the low participation factor of the higher modes. As can be seen in table 4.1.

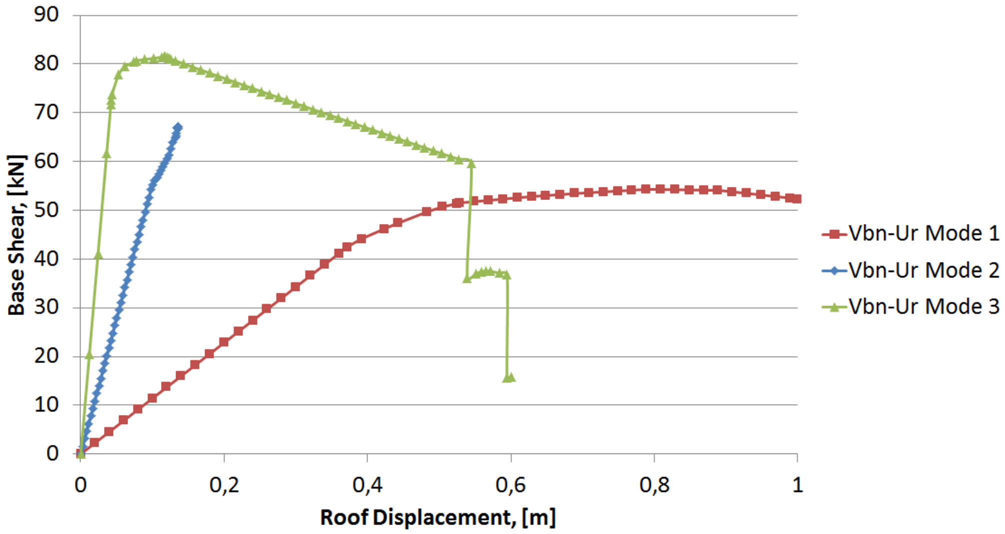

Figure 4.9: Pushover-curves for mode 1,2 and 3

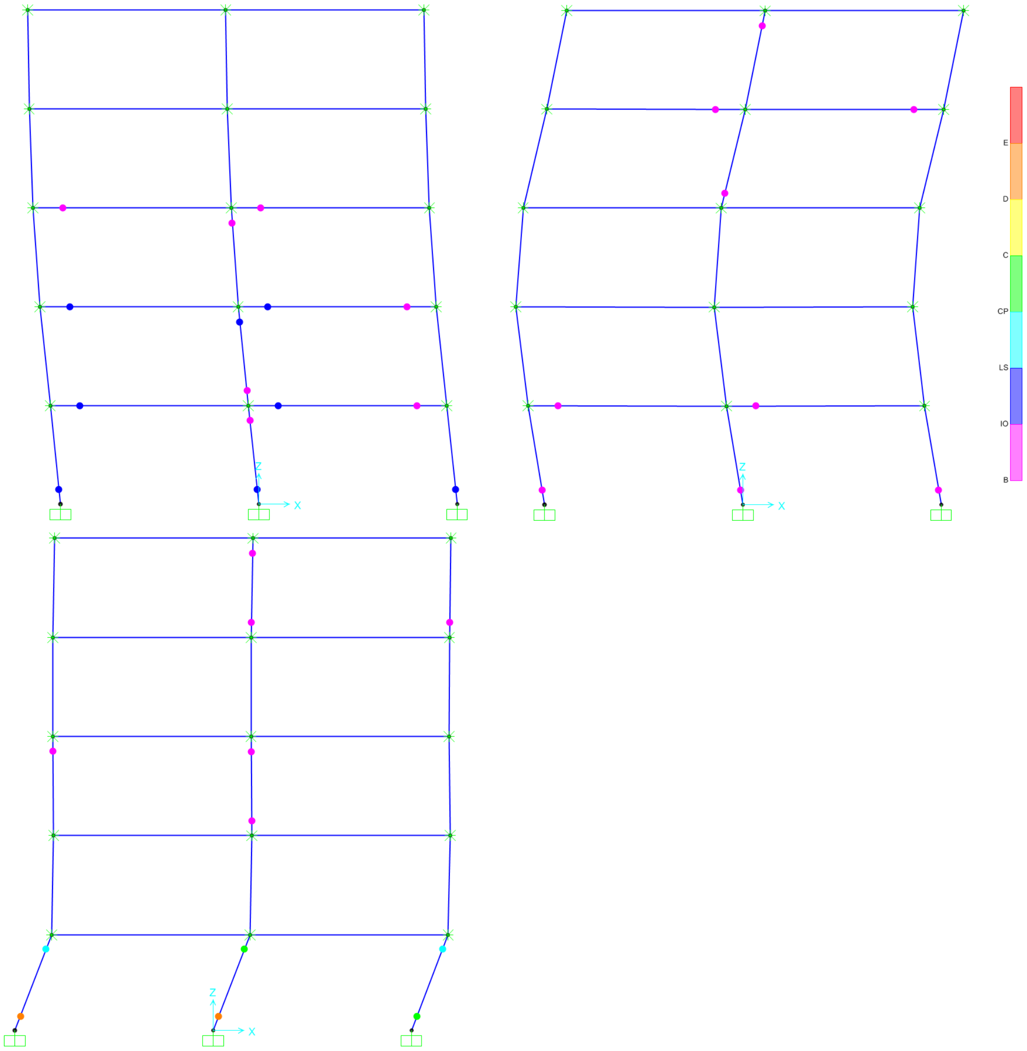
E
D
C
CP
LS
IO
B
Z
X

Figure 4.10: Plastic hinge formation

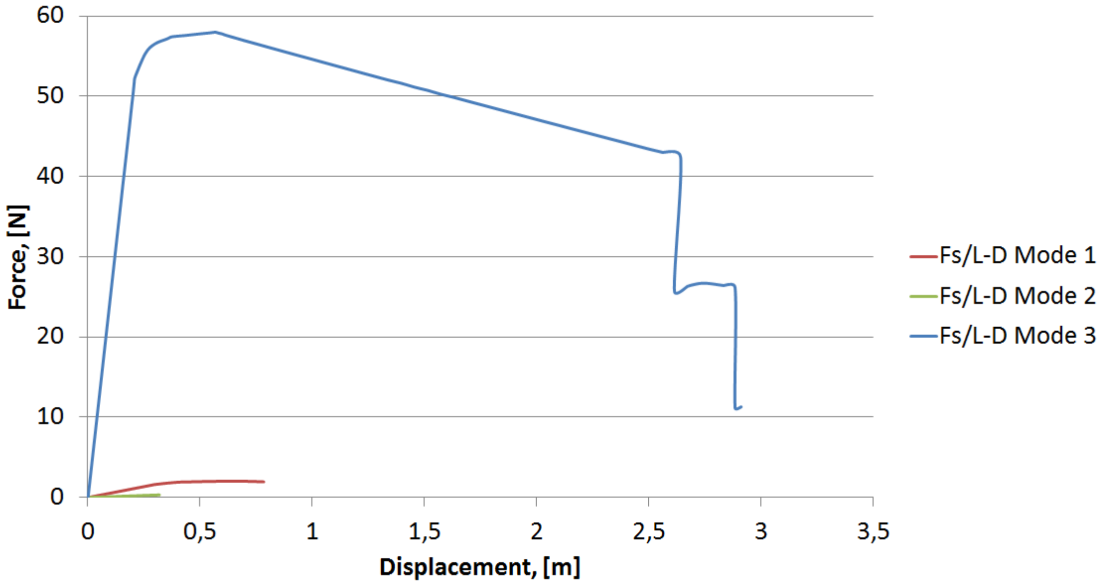

Figure 4.11: Force Displacement Curves for mode 1,2 and 3

Table 4.2: Comparison of elastic and inelastic periods

Mode	Elastic Period	Inelastic Period
Mode 1	2.4937 sec	2.7252 sec
Mode 2	0.7801 sec	0.7754 sec
Mode 3	0.4248 sec	0.3970 sec

Equation (4.13) is then used to transform the curves to the $F_{sn}/L_n - D_n$ relationship, and then equation (4.15) is used to find the inelastic period of the mode. The $F_{sn}/L_n - D_n$-curves are shown in figure 4.11 and the periods in table 4.2. The reason for the large difference between mode 3 and the other two modes is the fact that in the transformation, the base shear is divided by the modal participation factor squared. Since it is more than four times larger for mode 1, than mode 3, combined with the larger base shear to start with, a large difference is seen.

The periods acquired from this transformation are now used to find the SDOF displacement from the Eurocode 8 design spectrum. The spectrum is created using ground type B, with a ductility factor of 4. Ground acceleration is set to 0.3188 g and 0.4782 g, which is the maximum of the El Centro and El Centro x1.5 ground motion used earlier. The design spectrum is shown in figure 4.12. The different sections in the spectrum is defined as follows in equation (4.16) through (4.19) [11].

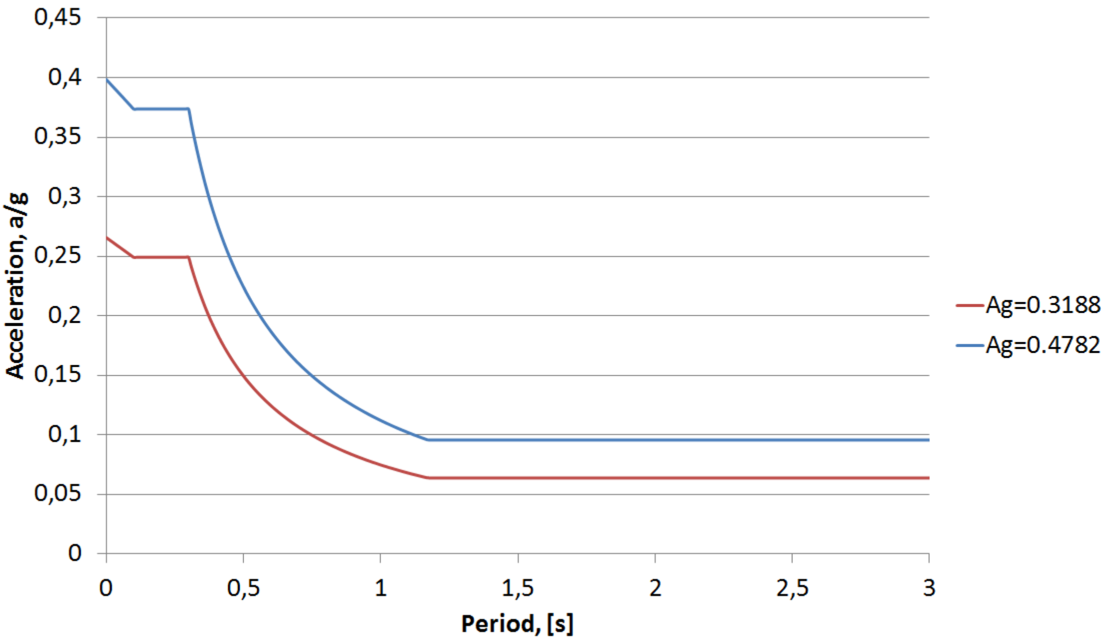

Figure 4.12: Design Spectrum from EC8 for ground acceleration 0.3188g and 0.4782g

Table 4.3: Modal Pushover Analysis Results

Mode	Period	PSA	D_n	U_r	V_{bn}
Mode 1	2.7252	0.06376 g	0.4471 m	0.6001 m	52.39 kN
Mode 2	0.7754	0.09642 g	0.0576 m	0.0245 m	13.98 kN
Mode 3	0.3970	0.19662 g	0.0308 m	0.0063 m	10.27 kN

$$0 \leq T \leq 0.1: \quad S_d(T) = a_g S\left[\frac{2}{3} + \frac{T}{0.1}\left(\frac{2.5}{q} - \frac{2}{3}\right)\right] \tag{4.16}$$

$$0.1 \leq T \leq 0.3: \quad S_d(T) = a_g S\frac{2.5}{q} \tag{4.17}$$

$$0.3 \leq T \leq 1.5: \quad S_d(T) \begin{cases} = a_g S\frac{2.5}{q}\left[\frac{0.3}{T}\right] \\ \geq 0.2a_g \end{cases} \tag{4.18}$$

$$1.5 \leq T: \quad S_d(T) \begin{cases} = a_g S\frac{2.5}{q}\left[\frac{0.3*1.5}{T^2}\right] \\ \geq 0.2a_g \end{cases} \tag{4.19}$$

Using the design spectrum from figure 4.12 and periods from table 4.2, combined with the relationship between pseudo acceleration and displacement, $D_n = A_n/(\omega_n^2)$ and $U_r = \Gamma_n \phi_{rn} D_n$. Table 4.3 is found. It can be noted that it is only mode 1 that goes into the inelastic range in both cases.

Using the modal combination method of SRSS to find the total, base shear turns out as 55.18 kN. Roof displacement turns out as 0.601 meters. Figure 4.13 shows the comparison

Table 4.4: Base Shear comparison MPA and NL-RHA

Method	Base Shear
MPA (3 modes), El Centro x1	55.10 kN
NL-RHA, El Centro x1	45.20 kN
MPA (3 modes), El Centro x1,5	60.39 kN
NL-RHA, El Centro x1,5	60.18 kN

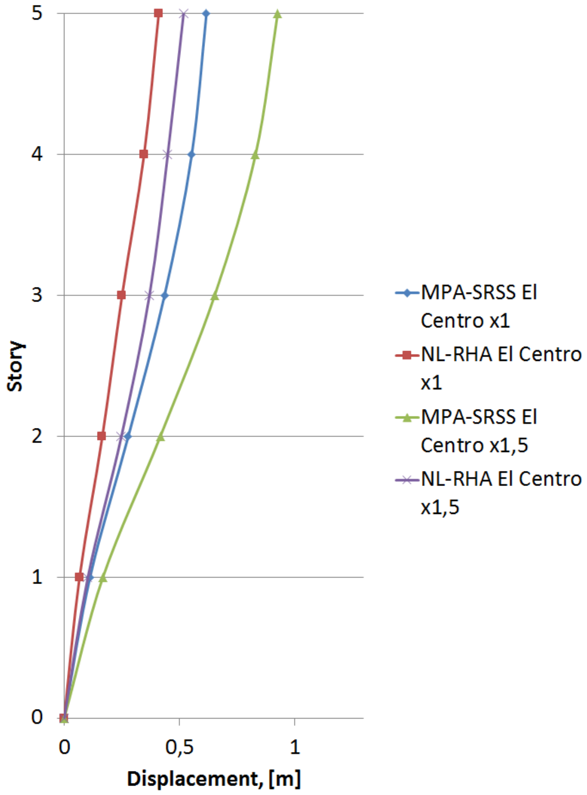

Figure 4.13: Floor Displacement comparison NL-RHA and MPA

of floor displacement between Non-Linear RHA and MPA. MPA overestimates the floor displacement, just as it overestimates the base shear. as shown in table 4.4.

Figure 4.14 shows the development of plastic hinges for the modal pushover analysis for mode 1 for the roof displacement found according to the 1.5x El Centro Design Spectrum and NL-RHA envelope. The NL-RHA has some more yielding in the top floors, while the MPA has some higher rotations in the lower part. This is due to the shape of mode 1. Mode 2 and 3 does not make any plastic hinges.

The results show that MPA combined with a design spectrum and NL-RHA gives similar values for base shear. The difference is 22 % for 1x El Centro and almost nothing for the 1.5x El Centro. There are larger differences in the floor displacement. This can be due to the fact that a design spectrum usually has higher spectral values than the response spectrum, causing higher acceleration values, and displacements. The errors are not to large, and considering the time saving that one will get with larger systems, it causes acceptable

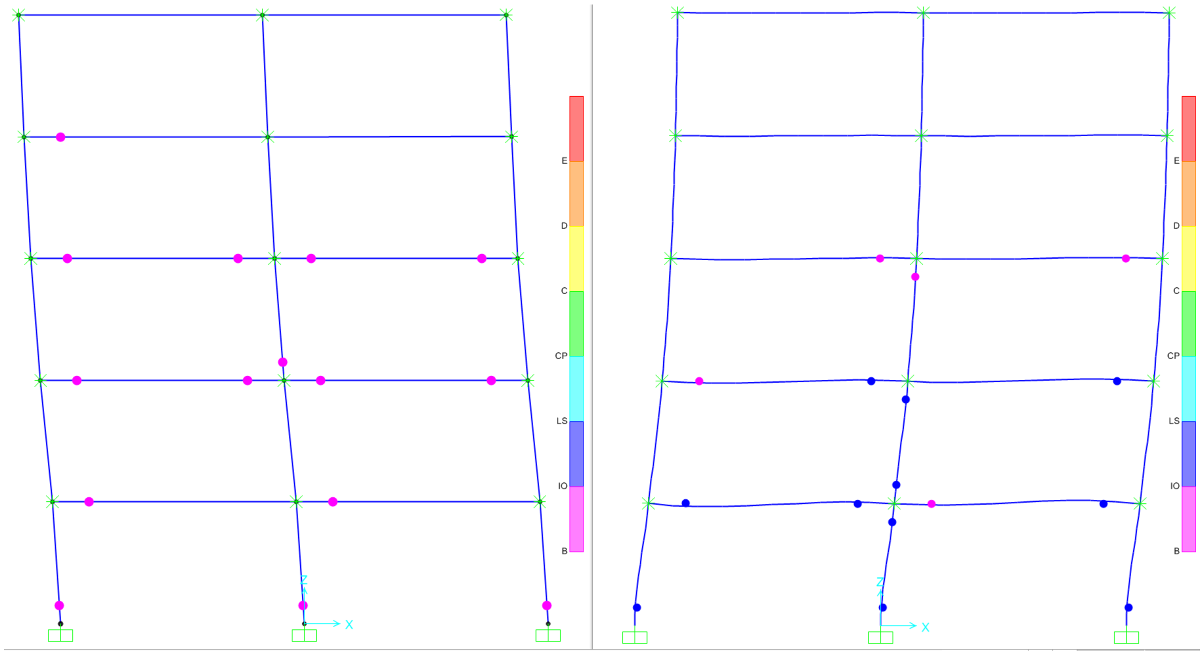
E
D
C
CP
LS
IO
B
Z
X
E
D
C
CP
LS
IO
B
Z
X

Figure 4.14: Development of plastic hinges, NL-RHA to the left, and MPA-mode 1 to the right

results. This is similar to the results found by Chopra and Goel in [9].

4.5 Modal Pushover Analysis for Asymmetric Plan Systems

This section will present the procedure developed by Chopra and Goel [12] to use modal pushover analysis to estimate the seismic demands for asymmetric buildings. The method will first be presented for elastic systems, and then for inelastic systems.

4.5.1 Elastic Systems

The lateral forces and torques are defined as follows

$$\mathbf{f}_{xn} = \mathbf{s}_{xn} A_n \quad \mathbf{f}_{yn} = \mathbf{s}_{yn} A_n \quad \mathbf{f}_{\theta n} = \mathbf{s}_{\theta n} A_n \tag{4.20}$$

The factors $\mathbf{s}_{xn}$, $\mathbf{s}_{yn}$ and $\mathbf{s}_{\theta n}$ are given by the following relationship

$$\mathbf{s}_n = \begin{bmatrix} \mathbf{s}_{xn} \\ \mathbf{s}_{yn} \\ \mathbf{s}_{\theta n} \end{bmatrix} = \Gamma_n \begin{bmatrix} \mathbf{m}\boldsymbol{\phi}_{xn} \\ \mathbf{m}\boldsymbol{\phi}_{yn} \\ \mathbf{I}_0\boldsymbol{\phi}_{\theta n} \end{bmatrix} \tag{4.21}$$

A_n is given as $\omega_n^2 D_n$ where D_n is the peak deformation of the nth mode elastic SDOF system. Static analysis of the system subjected to the forces listed in equation (4.20) will provide the peak value r_n of the nth mode contribution to the total response. The modal responses has then to be combined with a modal combination rule, preferably the CQC for asymmetric plan buildings. This is equal to standard RSA procedure.

4.5.2 Inelastic Systems

The procedure for asymmetric plans are quite similar to the symmetric method, with some differences. The structure is subjected to lateral forces and torques distributed over the structures height according to

$$\mathbf{s}_n^* = \begin{bmatrix} \mathbf{m}\boldsymbol{\phi}_{xn} \\ \mathbf{m}\boldsymbol{\phi}_{yn} \\ \mathbf{I}_0\boldsymbol{\phi}_{\theta n} \end{bmatrix} \tag{4.22}$$

These forces are used to develop the base shear-roof displacement, $V_{bn} - u_{rn}$. Chose the pushover curve in the direction of the dominant direction of motion in the mode. Gravity loads have to be applied before the pushover analysis. This curve is then idealized as a bilinear curve and converted to the force displacement relation $F_{sn}/L_n - D_n$ as shown in equation (4.13), where ϕ_{rn} is the value in the direction of the selected pushover curve, and M_n^* and Γ_n is in the direction of the ground motion.

The SDOF-system defined by the force deformation relation derived above, equivalent to the nth mode, is analysed to find the peak deformation D_n. The period is calculated as in equation (4.15). D_n can now be found by non-linear RHA or from a design/response

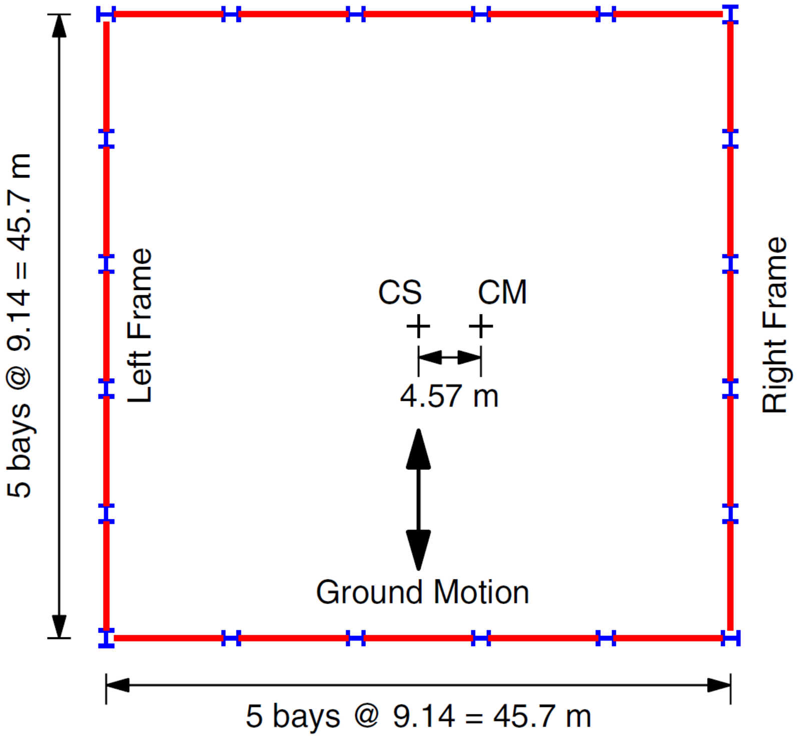

Figure 4.15: Plan of asymmetric plan building [12]

spectrum. The peak roof displacement is then found from $u_{rn} = \Gamma_n \phi_{rn} D_n$. This is repeated for as many mode as decided necessary, and then combined with CQC as described in section 3.1.2.

Chopra and Goel [12] also investigated the accuracy of this method on a 9-story SAC structure. They moved the centre of mass to make it asymmetric while maintaining its stiffness properties, a cross section is shown in figure 4.15.

3 different systems were chosen, to investigate different effects. The first one kept the I_{oj}/m-ratio equal to the symmetric plan building called U1. This caused a distinct difference between the period of the main torsional mode and lateral mode, as seen in figure 4.16. This is representative for perimeter moment resisting frames. The second model, U2, chose a I_{oj}/m that achieved very close modal periods, that can easily be seen in 4.16. The last system, U3, has an even larger I_{oj}/m-ratio making torsional rotations dominate the first mode, and lateral displacements in the 2nd mode, opposite of system one.

The system were analysed using the first 3 modal pairs. It is apparent that one modal pair is not enough, especially when it comes to story drift. Figure 4.17 shows how more modes improves the accuracy of the method for a symmetric plan, and the three system analysed in this section, compared to rigorous non linear response history analysis.

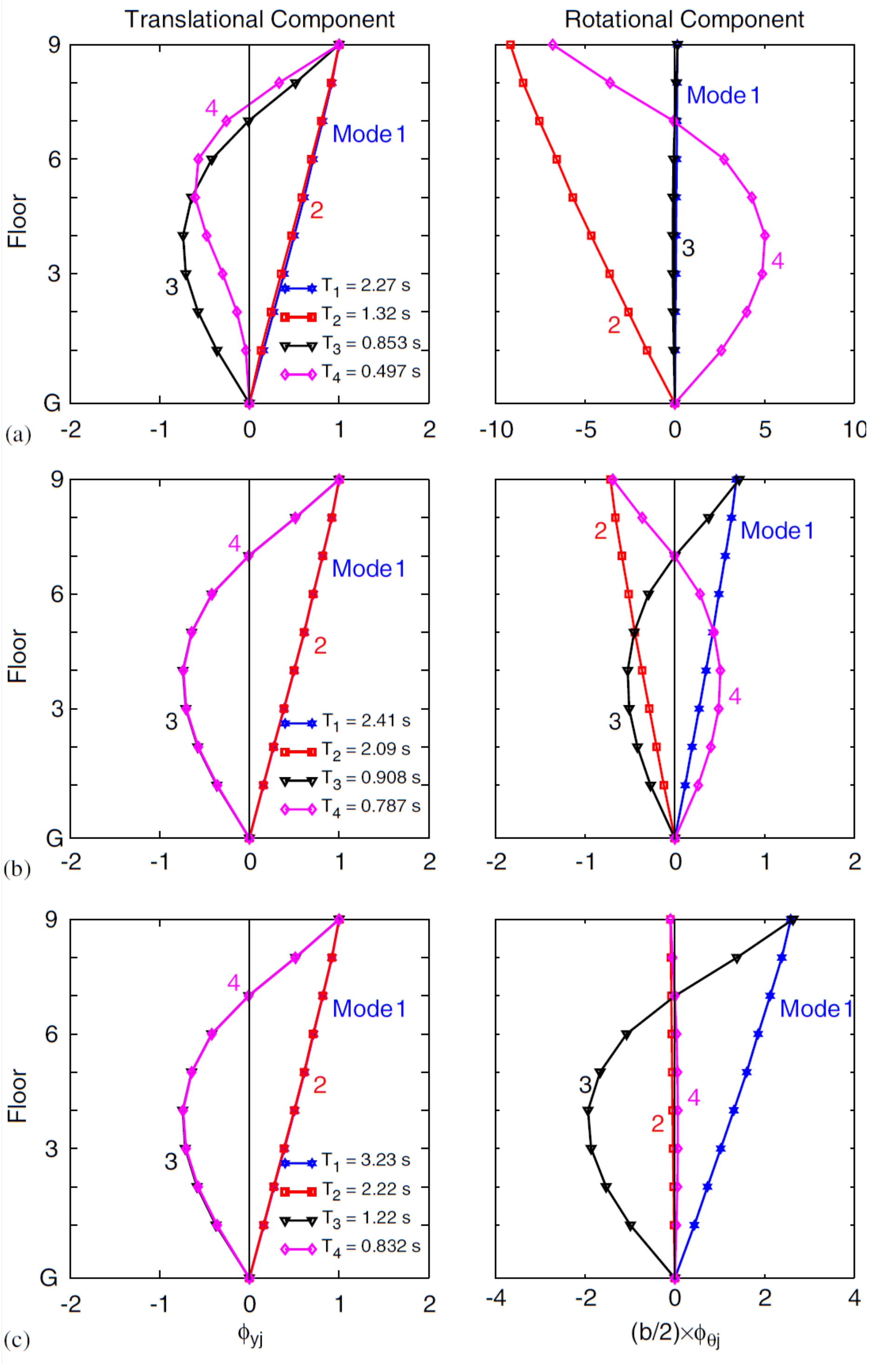

Figure 4.16: Mode shapes of systems [12]

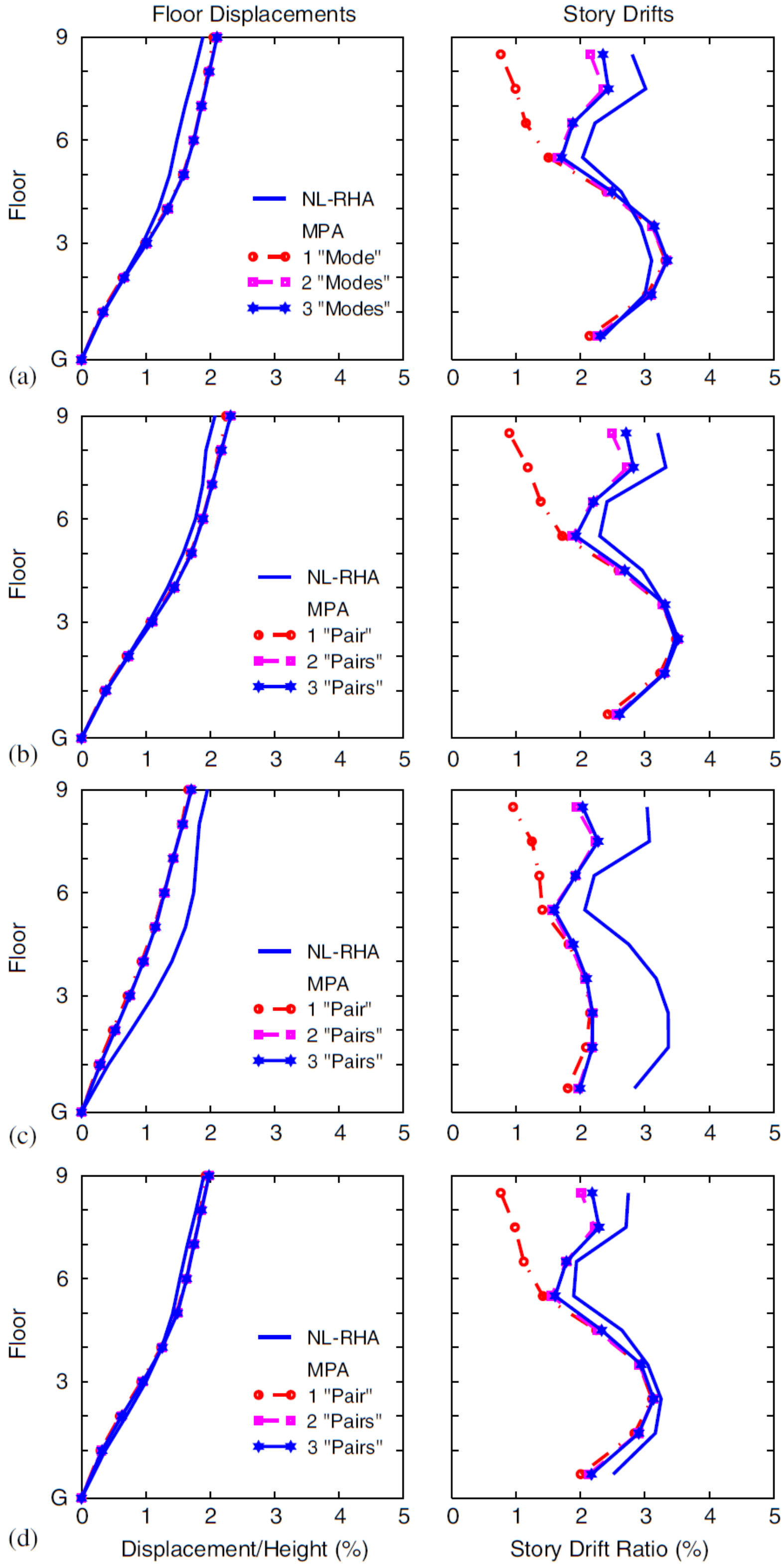

Figure 4.17: Floor Displacements and story drift demands for symmetric plan, U1, U2 and U3 [12]

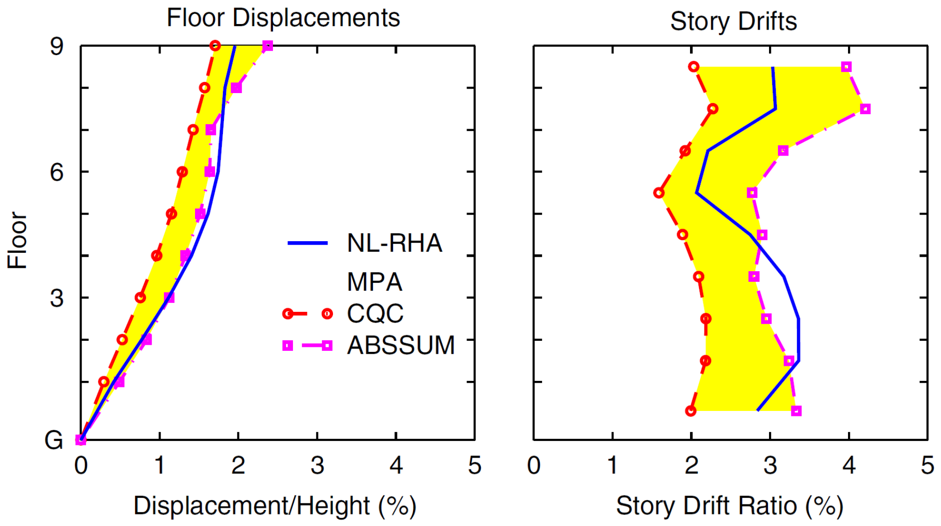

Figure 4.18: Floor Displacement and story drift comparison of CQC and ABSSUM [12]

An important observation of these results are the reduced accuracy of the 2nd system. Chopra and Goel assumes this is due to the fact that the maximums actually occurs at almost the same time, making ABSSUM a better modal combination method. This can be seen in figure 4.18

Chapter 5

Eurocode 8

This section will present demands that Eurocode 8 sets for Non-Linear Static analysis.

Section 4.3.3.4.1 states that the general rules demands that a bilinear force displacement relationship has to be used on every structural part. The elastic part of this bilinear relationship should be used as the secant stiffness to the yield point. The code allows for the post yield stiffness to be zero, or a trilinear relationship can also be used. The material parameters can be used as middle values calculated from characteristic values given in NS-EN 1992 to NS-EN 1996. The gravity load are to be included, but moments caused by $P - \Delta$-effects can be ignored unless it has a large influence on the behaviour of the structure. The seismic loads will be added in both positive and negative direction, and the largest results should be used.

5.1 Non-Linear Static Analysis (Pushover Analysis)

Section 4.3.3.4.2 contains the rules for this kind of analysis. The code states that if a structure fulfils the criteria for regularity in plan from section 4.2.3.2 or 4.3.3.1(8) a)-d), it can be analysed through two planar models, one for each horizontal direction. If these criteria are not fulfilled, a spatial model has to be adapted, where two independent analysis can be performed, one in each direction.

Section 4.3.3.4.2.2 demands that at least two vertical distributions of the lateral load has to be applied, namely a uniform pattern that is based on lateral forces which is proportional to the mass, independent of elevation, and a "modal" pattern which is proportional to the lateral force distribution found from elastic analysis. The loads are to be applied in the mass centre of the model, and accidental eccentricity, as presented in 4.3.2(1)P, should be taken into account.

When constructing the capacity curve, a displacement equal to 150% of the displacement defined in 4.3.3.4.2.6, and the overstrength factor is chosen as the lowest of the two lateral load cases. The determination of the displacement value follows in the subsection.

5.1.1 Determination of the Target Displacement for Non-linear Static Analysis (Pushover Analysis)

Appendix B in Eurocode 8 is an informative appendix that describes the codes requirements to find the target displacement. The notation in Eurocode 8 is different from the one used in the rest of the thesis, but in this section, the notation from EC8 will be used.

Section B.1 General states that the relationship between normalised lateral forces F_i and normalised displacements ϕ_i is

$$\bar{F}_i = m_i \phi_i \tag{5.1}$$

Where m_i is the mass of the ith story. The displacements are normalised so $\phi_n = 1$, where n is the control node, usually the roof, hence $\bar{F}_n = m_n$.

Transformation to an Equivalent SDOF-system

The mass of a SDOF system, m^* is determined as shown in equation (5.2)

$$m^* = \sum m_i \phi_i = \sum \bar{F}_i \tag{5.2}$$

and the transformational factor is given as

$$\Gamma = \frac{m^*}{\sum m_i \phi_i^2} \tag{5.3}$$

This equation is equivalent to the modal participation factor, given in equation (3.29).

The displacement d^* and force F^* for the equivalent SDOF system is calculated as shown in equation (5.4)

$$\begin{aligned} d^* &= \frac{d_n}{\Gamma} \\ F^* &= \frac{F_b}{\Gamma} \end{aligned} \tag{5.4}$$

F_b and d_n is base shear and displacement of control node respectively.

Determination of the Idealized Elasto-perfectly Plastic Force-displacement Relationship

The yield force F_y^* that represents the ultimate strength of the idealised system is equal to the base shear force when the plastic mechanism is formed. The idealised systems stiffness is determined so that the area under the deformation curve from both the actual and idealized

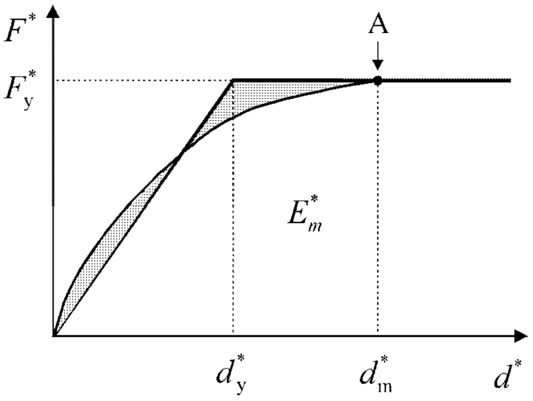

Figure 5.1: Determination of the idealized elasto-perfectly plastic force displacement relationship [11]

force are equal. Using this assumption, the yield displacement of the SDOF system d_y^* is given by equation (5.5)

$$d_y^* = 2\left(d_m^* - \frac{E_m^*}{F_y^*}\right) \tag{5.5}$$

Where E_m^* is the actual deformation energy needed to create the plastic mechanism. This is illustrated in figure 5.1

Determination of the Period of the Idealized Equivalent SDOF-system

The period T^* is defined in equation (5.6)

$$T^* = 2\pi\sqrt{\frac{m^* d_y^*}{F_y^*}} \tag{5.6}$$

This is equivalent to equation (4.15)

Determination of the Target Displacement for the Equivalent SDOF-system

The target displacement for a structure with unlimited elastic behaviour and period T^* is given by

$$d_{et}^* = S_e(T^*)\left[\frac{T^*}{2\pi}\right]^2 \tag{5.7}$$

Where $S_e(T^*)$ is the spectral value of the elastic acceleration spectrum at period T^*.

The calculation of d_t^* depends if the period is short or long, where periods higher than T_C are deemed as long.

1. If $T^* < T_C$
    - If $F_y^*/m^* \geq S_e(T^*)$ the response is elastic, and $d_t^* = d_{et}^*$

  - If $F_y^*/m^* \geq S_e(T^*)$ the response is non-linear and $d_t^* = \frac{d_{et}^*}{q_u}\left(1+(q_u-1)\frac{T_C}{T^*} \geq d_{et^*}\right)$, where $q_u = \frac{S_e(T^*)m^*}{F_y^*}$, the relationship between the acceleration in a infinitely elastic structure and a structure with limited strength.

2. If $T^* > T_C$, $d_t^* = d_{et}^*$

Determination of the Target Displacement for the MDOF-system

The target displacement is then given by

$$d_t = \Gamma d_t^* \tag{5.8}$$

Which is equivalent to (3.19), with $\phi_n = 1$.

This target displacement is then used to acquire the structural responses according to the capacity curve. The responses from each mode are then added together as described earlier to find the total response of the structure. This method is an expansion of the modal pushover analysis presented in section 4.4.

Chapter 6

Conclusion

It is clear from the information presented in this report, and in the community in general, that if a very accurate and precise result is wanted, there is no way around the non-linear response history analysis. This method does nonetheless bring with it some large complications, especially in the demand for computational power. The need to find a new stiffness, k, for each element in the system for each time step causes even a simple model as the one in section 3.2.3 to use over 45 minutes on one run, depending on how many members yielding. Considering a larger structure, and a need for the analysis to be run with 7 time series according to 4.3.3.4.3 in EC8, the computational resources needed are huge. Finding relevant time histories for the location chosen, can also be a challenge.

This is the reason alternative methods are needed. Modal pushover analysis saves a lot of computational time. Instead of solving each member at each time step of a acceleration time history, the structure is statically pushed to a given roof displacement with forces spatially distributed as the mode shapes. It also allows for the use of a design spectrum to provide the roof displacements, again saving time by not having to run 7 time histories. It is obviously not as accurate as NL-RHA, but for most uses accurate enough. It also discovers where plastic hinges are found, so it will be easy to control if the structure yields in the wrong places.

Both non-linear methods demands a lot of the model used. As described, a wrong model, simplified in the wrong places, can cause very different results compared to the real building. This is especially important in seismic loading, because when a section is designed to yield, and it turns out to be stronger than designed, it may cause the wrong part to yield, putting the whole structure in jeopardy.

In smaller structures it may not be worth the effort needed to construct a proper detailed model to investigate the effects of seismic loading, and elastic response spectrum analysis can be used with little effort.

Chapter 7

Further Work

Ideas for further work could be:

- Create hinge models that are more adapted to Norwegian situations than the FEMA 356
- Run the modal pushover analysis with a inelastic response spectrum instead of the Design Spectrum
- Further investigate the effects of modelling assumptions
- Investigate damping properties of different structures
- Investigate other method described in the community

Bibliography

[1] Mathisen, Kjell Magne *Lecture Notes, TKT4197 Non-linear Finite Element Analysis*, Fall 2011.

[2] Larkin, Tam, *Lecture notes, CIVIL720 Earthquake Engineering*, University of Auckland, New Zealand

[3] Chopra, Anil K. *Dynamics Of Structures.* Pearson Prentice Hall, 2007, Print

[4] El Centro Acceleration History. http://www.vibrationdata.com/elcentro.dat

[5] OpenSees Berkeley,
http://opensees.berkeley.edu/wiki/index.php/Hilber-Hughes-Taylor_Method

[6] CSIBerkeley, *https://wiki.csiberkeley.com/display/kb/Damping+coefficients*

[7] Chouw, Nawawi , *Lecture Notes, Civil 314 Structural Dynamics* Fall 2010, University of Auckland, New Zealand

[8] Gupta, A and Krawinkler, H. *"Dynamic P-delta effects for flexible inelastic steel structures*, Journal of Structural Engineering, ASCE, **126**: 145-154, 2000

[9] Chopra, Anil K. and Goel, Rakesh K. *"A modal Pushover analysis for estimating seismic demands for buildings"*, Earthquake Engineering And Structural Dynamics, **31**:561-582, 2002

[10] Gupta, A. and Krawinkler, H. *Behaviour of Ductile SMRFs at Various Seismic Hazard Levels"*, Journal of Structural Engineering, ASCE, **126**: 98-107, 2000

[11] Eurocode 8: Design of structures for earthquake resistance, Part 1: General rules, seismic actions and rules for buildings, Standard Norge 2005

[12] Chopra, Anil K. and Goel, Rakesh K. *"A modal Pushover analysis procedure to estimate seismic demands for unsymmetric-plan buildings*, Earthquake Engineering And Structural Dynamics, **33**:903-927, 2004

Appendix A

Response Spectrum

```
Ag=importdata('elcentro.txt');
for j=1:725
    T(1,j)=0.02*j;
    m=10;
    k(1,j)=((2*pi)^2*m)/(T(1,j)^2);
    c(1,j)=0.05*2*sqrt(m*k(1,j));
    a0=0;
    deltaT=0.02;
    gamma=0.5;
    beta=1/6;
    khat(1,j)=k(1,j)+(gamma/(beta*deltaT))*c(1,j)+(1/(beta*(deltaT)^2))*m;
    a(1,j)=(1/(beta*deltaT))*m+(gamma/beta)*c(j);
    b(1,j)=(1/(2*beta))*m+deltaT*((gamma/(2*beta))-1)*c(1,j);
    dD=zeros(length(Ag),1);
    dV=zeros(length(Ag),1);
    dA=zeros(length(Ag),1);
    D=zeros(length(Ag),1);
    V=zeros(length(Ag),1);
    A=zeros(length(Ag),1);
    dP=zeros(length(Ag),1);
    dPhat=zeros(length(Ag),1);
    for i=1:(length(Ag)-1)
        dP(i)=((Ag(i+1)*m)-(Ag(i)*m))*9.81;
        dPhat(i)=dP(i)+a(1,j)*V(i)+b(1,j)*A(i);
        dD(i)=dPhat(i)/khat(1,j);
        dV(i)=(gamma/(beta*deltaT))*dD(i)-(gamma/beta)*V(i)+deltaT*(1-↙
(gamma/(2*beta)))*A(i);
        dA(i)=(1/(beta*(deltaT^2)))*dD(i)-(1/(beta*deltaT))*V(i)-(1/↙
(2*beta))*A(i);
        D(i+1)=D(i)+dD(i);
        V(i+1)=V(i)+dV(i);
        A(i+1)=A(i)+dA(i);
    end
    Dmax(1,j)=max(abs(D));
    Vmax(1,j)=max(abs(V));
    Amax(1,j)=max(abs(A));
end
```

Appendix B

Elastic Analysis - Matlab

```
N=5; %Number of stories
g=9.81; %Gravity
h=3 %Height of stories
%M-Matrix

m=diag([6116.2 6116.2 6116.2 6116.2 6116.2]);
m

%K-Matrix
for n= 1:(N-1)
    k(n,n)=(2*3*12*210*10^9*6.06*10^-6)/3^3;
end

for n=N
    k(n,n)=(3*12*210*10^9*6.06*10^-6)/3^3;
end

for n=1:(N-1)
    k(n,n+1)=-(3*12*210*10^9*6.06*10^-6)/3^3;
end

for n=1:(N-1)
    k(n+1,n)=-(3*12*210*10^9*6.06*10^-6)/3^3;
end
k
%Eigenvalues
[modes wsquare]=eig(k,m)

T=zeros(N,1);
for n=1:N
    T(n)=(sqrt(wsquare(n,n))*(1/(2*pi)))^-1;
end
T

Modes=zeros(N,N);
for i= 1:N
    for j = 1:N
        Modes(j,i)=modes(j,i)/modes(N,i);
    end
end
Modes
%Generalized mass
Mn=zeros(N,1);
for i = 1:N
    for j = 1:N
    Temp=m(j,j)*(Modes(j,i))^2;
    Mn(i,1)=Mn(i,1)+Temp;
    end
end
Mn

Lhn=zeros(N,1);

for i = 1:N
    for j = 1:N
    Temp=m(j,j)*(Modes(j,i));
    Lhn(i,1)=Lhn(i,1)+Temp;
    end
end
Lhn

%Modal Participation Factor
GamN=zeros(N,1);

for i = 1:N
    temp=Lhn(i,1)/Mn(i,1);
    GamN(i,1)=temp;
end

GamN

Lnteta=zeros(N,1);

for i = 1:N
    for j=1:N
        temp=144*j*m(j,j)*Modes(i,j);
        Lnteta(i,1)=temp+Lnteta(i,1);
    end
end
Lnteta

%Insert Displacement from Response Spectrum
D=[(1.992)/wsquare(1,1) (8.1)/wsquare(2,2) (7.7)/wsquare(3,3) (5.6)/wsquare↙
(4,4) (7.59)/wsquare(5,5)]

%Story Displacements
for i= 1:N
    for j = 1:N
        u(j,i)=GamN(i)*Modes(j,i)*D(i);
    end
end

u
%SRSS Displacement
usum=zeros(N,1);
for i = 1:N
    for j = 1:N
    temp=(u(i,j))^2;
    usum(i,1)=usum(i,1)+temp;
    end
    usrss(i,1)=sqrt(usum(i,1));
end
usrss


%Acceleration from Response Spectrum
A=[1.992 8.1 7.7 5.6 7.59]
%Story Forces
for i=1:N
    for j = 1:N
```

```
        f(j,i)= GamN(i)*m(j,j)*Modes(j,i)*A(i);
    end
end
f

%Base Shear
Vb=zeros(N,1);
for i= 1:N
    for j = 1:N
        Temp=f(j,i);
        Vb(i,1)=Vb(i)+Temp;
    end
end
Vb

%Base Shear SRSS
Vbs=0;
for i = 1:N
    Temp=(Vb(i,1))^2;
    Vbs=Vbs+Temp;
end
Vbsrss=sqrt(Vbs)


Mb=zeros(N,1);
for i= 1:N
    for j = 1:N
        Temp = f(j,i)*h*j;
        Mb(i,1)=Mb(i,1)+Temp;
    end
end
Mb
```

Appendix C

Correlation Coefficient

```
omega=[3.450248;2.97132;1.509088;1.16982;1.01603;0.728498;0.640462;0.5561;↙
0.514713;0.49744;0.480185;0.435423;]
zeta=0.05
betain=zeros(12,12);
for i=1:12
    for j=1:12
        betain(i,j)=sqrt(omega(i)^2)/sqrt(omega(j)^2);
    end
end
betain

roin=zeros(12,12);
for i=1:12
    for j=1:12
        roin(i,j)=(8*zeta^2*(1+betain(i,j))*betain(i,j)^(3/2))/((1-betain↙
(i,j)^2)^2+4*zeta^2*betain(i,j)*(1+betain(i,j))^2);
    end
end
roin

zeta2=0.2

roin2=zeros(12,12);
for i=1:12
    for j=1:12
        roin2(i,j)=(8*zeta2^2*(1+betain(i,j))*betain(i,j)^(3/2))/((1-betain↙
(i,j)^2)^2+4*zeta2^2*betain(i,j)*(1+betain(i,j))^2);
    end
end
roin2
```